ABSTRACT

STRUCTURE AND DYNAMICS OF SOLUBLE GUANYLYL CYCLASE

by
Kentaro Sugino

Soluble guanylyl cyclase (sGC) is one of the key enzymes involved in many fundamental biological processes including vasodilatation. It can be allosterically activated by synthetic compound such as YC-1. Recently, the 3D structure of adenylyl cyclase (AC), which is a homologue of sGC, was determined. Using AC as template and homology modeling, the 3D structure of sGC is predicted. Prior experimental work has suggested two binding modes of YC-1. In the current investigation, molecular dynamics simulations (MD) were conducted to seek more detail of molecular mechanism of sGC activation.

From these MD simulations, a tentative mechanism of sGC activation is established. The difference in the initial binding modes of YC-1 in its binding pocket results in different conformational changes in the active site of sGC, which results in different catalytic capability. Meanwhile, YC-1 was found to be strongly attracted to α_1 CYS594, a residue deep inside of the allosteric binding pocket.

STRUCTURE AND DYNAMICS OF SOLUBLE GUANYLYL CYCLASE

by
Kentaro Sugino

A Thesis
Submitted to the Faculty of
New Jersey Institute of Technology
in Partial Fulfillment of the Requirements for the Degree of
Master of Science in Computational Biology

Department of Computer Science

May 2005

APPROVAL

STRUCTURE AND DYNAMICS OF SOLUBLE GUANYLYL CYCLASE

Kentaro Sugino

Dr. Marc Qŭn Ma, Master Thesis Advisor — Date
Assistant Professor of Computer Science, NJIT

Dr. Frank Y. Shih, Committee Member — Date
Professor and Associate Chairperson of Computer Science, NJIT

Dr. Alexandros Gerbessiotis, Committee Member — Date
Associate Professor of Computer Science, NJIT

BIOGRAPHICAL SKETCH

Author: Kentaro Sugino

Degree: Master of Science

Date: May 2005

Undergraduate and Graduate Education:

- Master of Science in Computational Biology,
  New Jersey Institute of Technology, Newark, NJ, 2005

- Bachelor of Art in Literature,
  Waseda University, Tokyo, Japan, 1996

Major: Computational Biology

To my beloved family

ささやかな成果だけど、いろいろと支えてくれた父さんと母さん、
留守を守ってくれた祥太郎にこの論文を捧げます。

ACKNOWLEDGMENT

I would like to express my deepest appreciation to Dr. Marc Qun Ma, who not only served as my thesis advisor, but also constantly gave me various support, encouragement, challenging task, keen insight, positive attitude, and his enthusiastic emotion for education and research. Special thanks are given to Dr. Frank Y. Shih and Dr. Alex Gerbessiotis for actively participating in my committee, and to Dr. Annie Beuve for exposing such an exciting research topic to my research group.

I also wish to thank Yu Wang for his collaboration, assistance and kind friendship over the years.

TABLE OF CONTENTS

TABLE OF CONTENTS
(Continued)

Chapter **Page**

TABLE OF CONTENTS
(Continued)

Chapter **Page**

LIST OF TABLES

LIST OF FIGURES

LIST OF FIGURES

LIST OF FIGURES
(Continued)

LIST OF FIGURES
(Continued)

Figure **Page**

CHAPTER 1

INTRODUCTION

1.1 Objective

The objective of this project is to reveal the mechanisms of allosteric activation of soluble guanylyl cyclase (sGC) and guanosine 5'-triphosphate (GTP) complex by using molecular dynamics (MD) simulation. More specifically, the pre-chemistry conformational changes induced by allosteric activators such as 3-(5'-hydroxymethyl-2'-furyl)-1-benzylindazole (YC-1) and the mechanisms of binding mode selectivity will be investigated by using bio molecular modeling and multiscale simulations, which will lead to in-silico theories that describe the mechanism of the allosteric activation.

The sGC complex has been widely investigated especially in this decade, and it is well known as an important component of signal transduction pathway in such as smooth muscle cell in vascular systems. Thanks to lots of scientific effort, it is revealed that sGC binds to nitoric oxide (NO) and carbon monoxide (CO) then turns GTP into guanosine 3',5'-cyclicmonophosphate (cGMP), and the cGMP acts as secondary messenger signal molecule. Furthermore, when a catalytic compound such as YC-1 is added in the system, the reaction will be activated ten to hundreds folds. Therefore to reveal this complex molecular mechanism leads to discovering new potential drug/therapy agents for such as high blood pressure disease. However, in spite of the recognition of the importance and numerous scientific efforts, which have been already paid, the detail of molecular mechanism of sGC, GTP and YC-1 complex is still unclear.

Partly because, unfortunately, although there are plenty of effort and progress in science, to measure specific atomic distance or to visualize the molecular motion, conformational change are still difficult to achieve in laboratory experiment. Meanwhile, 3D structure of sGC is still not available. One possible solution is computational simulation with molecular dynamics approach. In this investigation, several molecular dynamics simulations were conducted to aim to reveal the molecular mechanism of sGC, GTP and YC-1 complex. Those molecular dynamics simulations were conducted on three systems. These three systems were designed based on collaborator's achievement, which are lab experimental work conducted by Dr. Beuve's research group [1]. NAMD program suite [7] for molecular dynamics simulation and VMD program suite [8] for visualization were employed. To determine potentials, MOPAC program suit [9] for semi empirical quantum calculation was employed. For initial geometry optimization of YC-1, atomic coordinates data was submitted to PRODRG server [10]. The analysis was conducted mainly by measuring and comparing the distance between the alpha carbons in those selected amino acids. XMGRACE program suit, and Microsoft Excel program suit were employed for plotting purposes. VMD, namdplot, and custom perl class library were employed for generate and extracting atomic distance data sets.

1.2 Related Background of Biology and Computing

1.2.1 sGC, GTP and YC-1 Complex

sGC is one of the important molecules in biological system's signal transduction pathway and has been widely investigated. It is a 150 kDa heterodimer enzyme, consisting of the α_1 (74-82 kDa) subunit and β_1 (69-74 kDa) subunit [4-6]. Very basic function of the

molecule is, as it's name stands for, turning GTP into cGMP, and then the cGMP works as signaling molecule. sGC can be activated allosterically by synthetic compounds such as YC-1, 3-(5'-hydroxymethyl-2'-furyl)-1-benzylindazole [2, 3], its derivatives and some other compounds. That activation boosts up its catalytic function. In spite of the recognition of its importance and lots of scientific effort, which has been paid so far, there is limited success in understanding the mechanisms of the regulation of sGC [1, 11-14].

The sGC has several functional and structural features in common with adenylyl cyclase (AC) [15]. It is generally accepted that catalytic centers of AC and sGC are homologous [16]. As sGC catalyzes the cyclization of GTP, AC catalyzes the cyclization of ATP, and GTP and ATP are chemically related substrates, have very similar structure. As binding and catalysis occur in the COOH-termini of the α_1 and β_1 subunits of sGC, those events occur in the C_1 and C_2 sub domains of AC.

Recently the 3D structure of active form of AC was determined [17]. It revealed that there are two binding pockets, which are formed at the interface of C_1 and C_2 domains, and extensive contacts between the two domains occur. One pocket is the binding site where ATP binds and catalysis takes place. The other is the regulatory site where forskolin (FSK), an allosteric activator of the AC binds. Because of this achievement, homology modeling of sGC becomes possible.

Modeling of sGC revealed a similar structural organization [16]. The association of the COOH-termini of α_1 and β_1 subunits results in the formation of the GTP binding pocket and a putative second pocket that corresponds to the FSK site of AC. This second pocket is pseudosymmetric and homologous with the GTP binding pocket but lacks

residues that are critical for substrate catalysis [18], so it may not GTP pocket. The structural homology of AC and sGC suggests that these two enzymes are functionally similar. Naturally, this leads to the idea of that the pseudosymmetric binding pocket of sGC has a very similar allosteric function of the AC's FSK binding pocket, and thus a logical site for YC-1 binding [2]. In AC, the binding event of FSK brings out conformational change and turns AC into more favor form of its activity by increasing the affinity between C1 and C2 at the interface contact regions [17, 19]. A recent mutational analysis supports this model, and three residues, V506, K1014 and P1015 are identified as critical for contacts between the two subunits of AC [20]. As it referred as homology, the residues and secondary structures that shape the interface between the C_1 and C_2 domains are conserved in the α_1 and β_1 subunits of the sGC. Again, it is naturally suggesting that interface contacts are critical for transduction of signals of activation of sGC, and there would be critical residues in α_1 and β_1 subunits. The experimental studies were conducted, and several critical residues and potentially critical residues were identified [1].

1.2.2 Classical Molecular Dynamics

MD is a venerable computer simulation technique in bio-molecular modeling that interfaces mathematics, biology, chemistry, physics and computer science [38]. MD faithfully models the constituent atoms in bio-molecules that continuously interacting with themselves and the environment. In classical MD, starting with the atomic coordinates, connectivity and force field parameters, one computes trajectories, in other word, collections of the time evolution of the Cartesian coordinates for each atom in three

dimensional space. MD is also known to be very compute-intensive. Modern bio-molecular MD simulations may take months to finish [39, 40]. Key methods for speeding up MD simulations include using multiple time stepping (MTS) (quasi-)multiscale integrators, parallel computing, fast electrostatics, and well-designed software.

A popular solver for the MD equations is the Verlet-I [42]/r-RESPA [41]/Impulse MTS algorithm, which splits the potentials into fast (harmonic, dihedral and improper, and short-range Lennard Jones and electrostatic) and slow (long-range electrostatic) components, and evaluates the former more frequently than the latter. MTS integrators allow larger time steps (in outer integrators) than their single time stepping (STS) counterparts (the Verlet or Leapfrog integrators), thus reducing the time for computing the long-range electrostatic forces, which are the most compute-intensive among all the forces. These long-range electrostatic forces play a critical role in simulations of biological events such as protein folding/unfolding and ligand-receptor binding [43], and therefore it is crucial to include these forces. The Impulse algorithm has good long-time energy behavior. Due to the strong nonlinearity of non-bonded forces and extreme stiffness of the governing equations in MD, the outer time steps allowed are restricted to less than 3.3 femtoseconds in the Impulse integrator for most biological systems, so as to obtain stable solutions over a long period of simulated time. The restriction of time steps in MTS integrators is due to 3:1 nonlinear overheating [44, 45].

Classical molecular dynamics assumes, 1) acceptance of Born-Oppenheimer approximation, 2) nuclei move on a single potential surface, 3) the potential surface can be approximated by an empirical fit, 4) then nuclear motion can be described by classical

mechanics [21]. Therefore basically classical molecular dynamics skips to calculate those of quantum events, so it will not simulate bond formation/breaking, electron transition and those of chemical events. However, it is widely accepted as a powerful tool for deep understanding of the molecular mechanism and kinetics of "before-chemistry" and "after-chemistry", and as a matter of fact, lots of MD simulation have showed quite good match with theory and results of laboratory experiments in many systems.

1.3 Research Design

Although classical molecular dynamics (MD) simulation does not simulate those of chemical reaction events such as electron donation/acceptation, bond formation/breaking and so on, it is widely accepted that MD calculation reflects quite reasonably the state of real world phenomenon and theory if it is conducted under proper condition and system design. At least, MD calculation reflects classical Newton's dynamics property of given system, and it would be valuable clue to understand targeted molecular complex's mechanism. Therefore MD approach was chosen for this investigation.

There are many available MD program packages. From those of program packages, NAMD program suite [7], was chosen for this investigation because it has wide scalability, specific features such as interactive MD, which might be used in later analysis, and it accepts CHARMM [23] force field parameters, which is well known and accepted as one of the best parameter sets especially for bio molecular simulation. Since sGC's 3D structure has not been determined yet, homology modeling was conducted by using Adenylyl Cyclarse as a template. Several more information will be described in Chapter 3. For explicit solvate model, TIP3P water model was employed. In this model,

water model is dealt as a sort of sticky triangle, rather than allowing vibration of two hydrogen atoms. From the stand point of Quantum mechanics, this is not true model, however the fact that this model shows very good match with laboratory experiment result, is commonly accepted in MD community.

1.4 Three Model Systems

Lamothe et al. [1], the collaborators of this investigation, addressed the possibility of that YC-1 might have two binding mode in sGC, one is normal mode in which YC-1's hydroxymethyl group face to inside of the binding pocket and the other is flip mode in which the hydroxymethyl group face to outside of the binding pocket. Their data imply that those two possible modes have different effect in the potentiation of GTP cyclization. In this investigation, System B refers to normal binding mode and System C refers to flip binding mode. Along with these two systems, as for basal activity of sGC complex with GTP but without YC-1, another system, System A was also constructed under same condition except that YC-1 was not included.

1.5 Basic Procedure of MD Simulations

Figure 2.1 shows basic procedure for the MD simulation in this investigation. After building initial coordinates, the model was solvated using TIP3P water box. Then MD configuration was determined, and simulation was run for certain time steps. After MD simulation, the output files including energies and DCD trajectory file analysis was. To measure conformational changes, especially in binding pockets, and inter sub unit association, several C α's of amino acids near contact region of sGC were chosen.

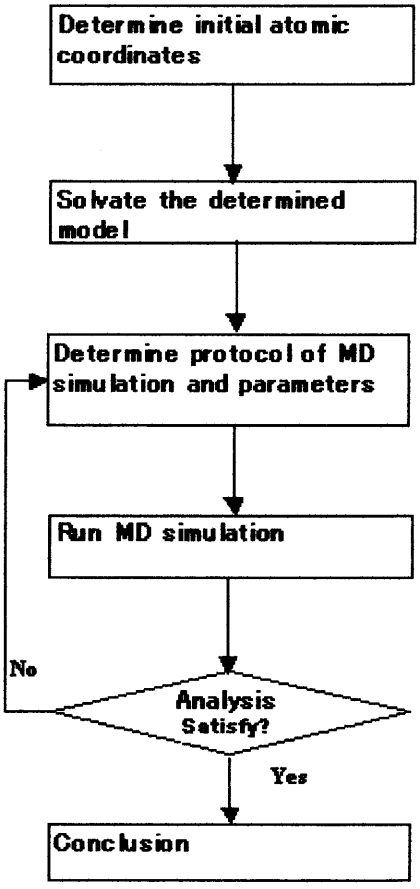

Figure 1.1 Basic procedure for MD simulation.

CHAPTER 2

BUILDING MODEL SYSTEMS FOR MD SIMULATION

2.1 Homology Modeling of sGC

Although the amino acid sequence of sGC was already determined, its three dimensional 3D structure has not been determined yet. However, in late 1990's Tesmer et al. [17] succeeded in crystallizing adenylyl cyclarse (AC), which is a homology protein of sGC with high sequence similarity. Figure 2.1 shows the result of sequence alignment of the α_1 subunit of sGC and C_1 subunit of AC. It shows the sequence identity is 57%. Their achievement allows molecular modeling community to conduct homology based modeling of sGC. An initial homology modeling based on AC atom coordinates. AC atom coordinates were obtained from PDB entry (ID: 1azs), then based on these coordinates, three parts of sGC amino acid sequences were coordinated with Insight Ⅱ program suite. Those three parts are α_1 V480-L625, β_1 V420-L485 and β_1 H492-E576 [1], which correspond to the catalytic center of the sGC. This homology-based model was used for initial investigation. More research is on going in order to improve this model. The predicted structure of the catalytic center of sGC is shown in Figure 2.2.

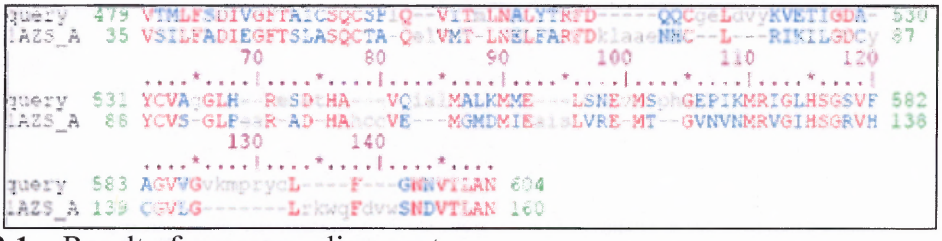

Figure 2.1 Result of sequence alignment.

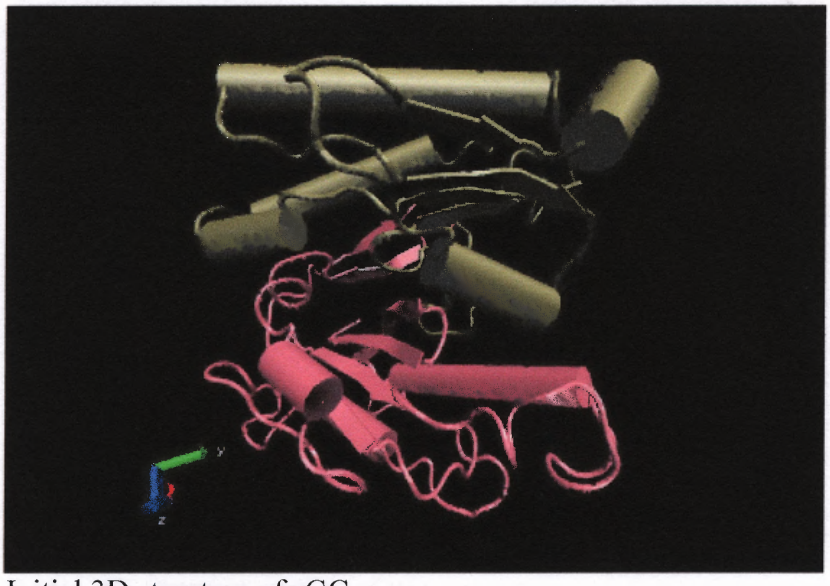

Figure 2.2 Initial 3D structure of sGC.

2.2 Generating Initial Simulation Base System with VMD

Solvation of the proteins is needed to mimic the biological environment before any production MD run since proteins function in water environment. As it was mentioned in previous chapter, in this investigation, TIP3P water model was employed as explicit solvent. VMD has plug-in package to put target molecule into water solvent. This plug-in package, named solvate, is controllable via both VMD GUI console and VMD command line mode. Appendix A is very simple short tcl script to use solvate and put a target molecule into water solvent box. In this investigation, sGC complex was put into 3Å water layer box from outmost its surface. Figure 2.3 shows generated base system, sGC complex (dark brown: α_1 sub-unit, pink: β_1 sub-units) placed in water box.

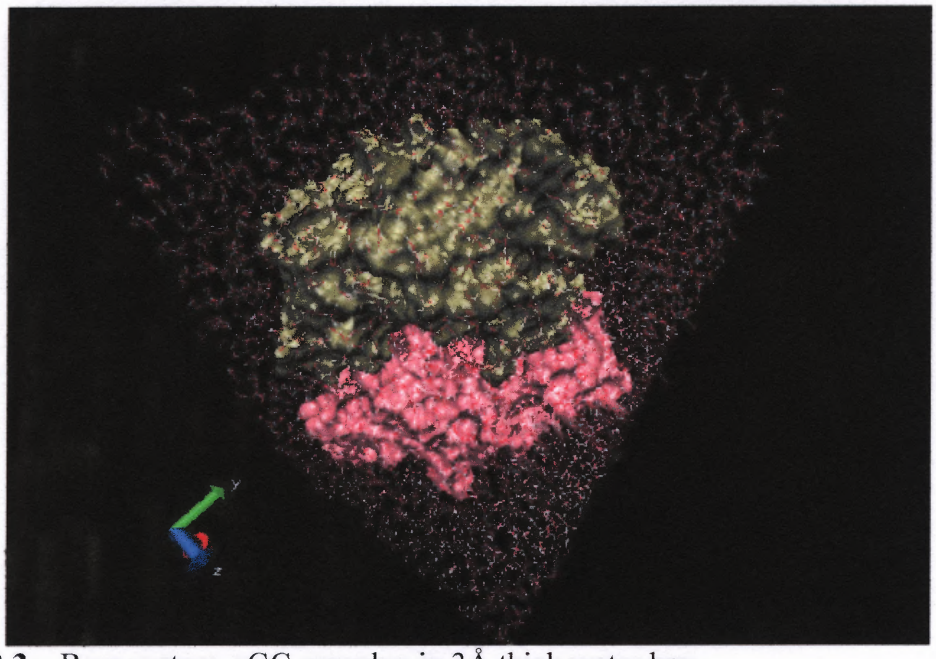

Figure 2.3 Base system, sGC complex in 3Å thick water box.

2.3 Parameterization of GTP and YC-1

2.3.1 GTP Topology File

GTP is one of the key players in this investigation, however there is no standard GTP parameter in CHARMM [23] entry. Fortunately, in downloadable CHARMM parameters, there is ATP entry (toppar_all27_na_nad_ppi.str), and guanine entry too. The difference between ATP and GTP is just base parts. Parameterization of GTP is done by replacing adenosine in ATP with guanine and using the parameters of the tail of ATP (the Phosphor groups) and guanine. Appendix C is quick recipe to prepare GTP topology file. This is basically same procedure, which is described in one of the NAMD/VMD tutorial, "Topology file tutorial" [25].

2.3.2 Brief Introduction to MOPAC

There is no standard YC-1's parameter too and similar structure in CHARMM entry is very limited. Therefore, parameter determination procedure was conducted. In official NAMD site, there is a tutorial document that deals with parameter determination of novel residue ("Parameterizing a Novel Residue" [26]). According to this tutorial, to obtain precise parameters such as equilibrium bond length, angles, and energetic barriers, full ab-initio calculation with GAMESS [27] or GAUSSIAN [28] software suites is preferred. Another choice is to conduct calculation by semi-empirical package. One of the advantages of semi-empirical calculation is its fast calculation. Therefore semi-empirical freely available quantum chemistry calculation software, MOPAC, was employed. Along with the software, the molecule's structure information was submitted to PRODRG2 [10] server with energy minimize option. MOPAC is widely used software in computational chemistry community. The development of MOPAC started from 1980's by Dr Stewart, and continuously is improved [9]. MOPAC employs Molecular Orbital Theory [33, 34, 35], and calculates optimized geometry (bond length, angle, dihedral angle), electron density, atomic charge, and lots of other molecular aspect. The major difference between semi-empirical approach (MOPAC) and ab-initio approach (GAMESS, GAUSSIAN) is while ab-initio approach calculates Hartree-Fock equation without mathematical approximation or any pre-defined parameters as long as possible, semi-empirical approach uses ready-made parameters for the calculation. Advantage of semi-empirical model is 1) Fast, 2) It allows to calculate relatively large molecule, 3) Sometime it gives very accurate output as same as ab-initio approach. Limitation is accuracy and the output is always depending on initial input parameter.

2.4 Initial Input Coordinate File and PRODRG Server Submission

This procedure started from the atomic coordinate file of YC-1 in PDB format, which ware generated with Insight-Ⅱ program suit, and energy minimized along with sGC complex. Because the structure minimized as a part of whole system (sGC, YC-1, Mg++ ions, and GTP in 5A water shell), it could be non-minimized state. Figure 2.4 shows YC-1's initial structure. Figure 2.5 is same YC-1 structure but its side view. Note, from side view YC-1 is in such almost plane shape. The initial structure was submitted to PRODRG2 server with energy minimize option. Then, the server succeeded to generate energy-minimized topology in PDB format. To obtain more precise ESP and optimized structure, MOPAC calculation was conducted against this new structure. MOPAC accepts z-matrix format file. There are lots of freely available z-matrix editor, such as MOLKEL [29], MOLDEN [30], and Winmoster [31]. Most of those editors can convert PDB format file into z-matrix format. For here, MOLDEN was employed and generated z-matrix. MOPAC calculation was conducted by using PM3 method [32]. Figure 2.6 shows comparison of these three structures (white; initial structure, red; PRODRG2 generated, green; MOPAC generated). As Figure 2.6 shows, PRODRG2 and MOPAC generated structure was very similar to each other. The major difference between those two and initial structure is the bend angle of benzene ring. Therefore, the MOPAC generated structure's topology and calculation result were employed as starting point of new parameter determination.

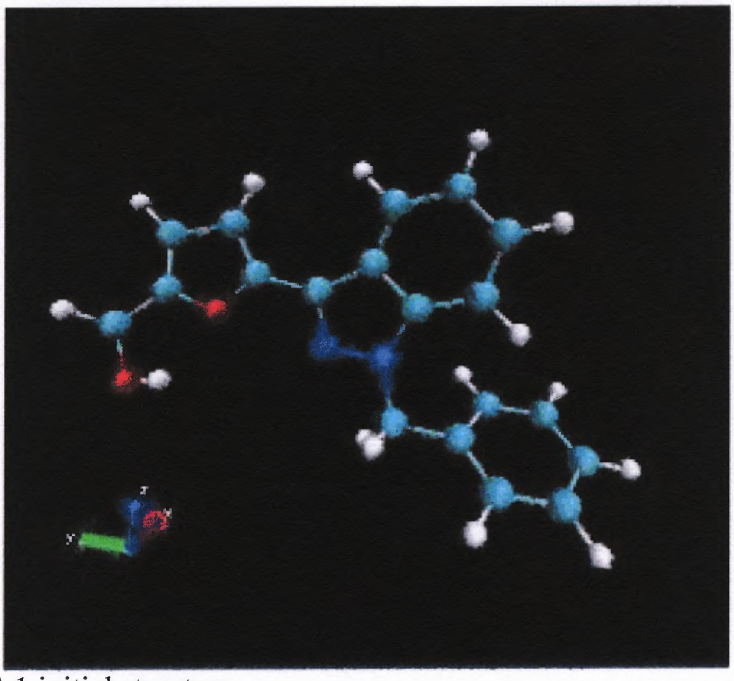

Figure 2.4 YC-1 initial structure.

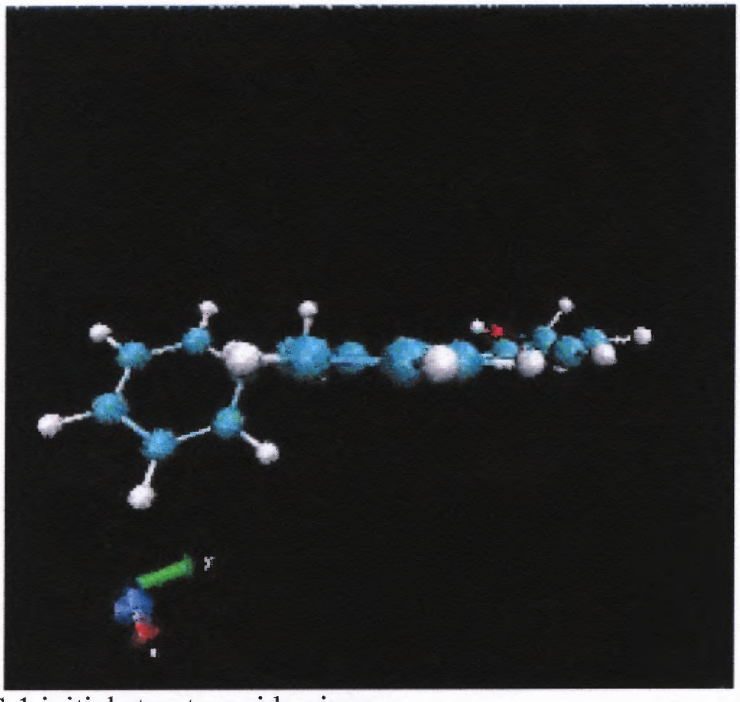

Figure 2.5 YC-1 initial structure side view.

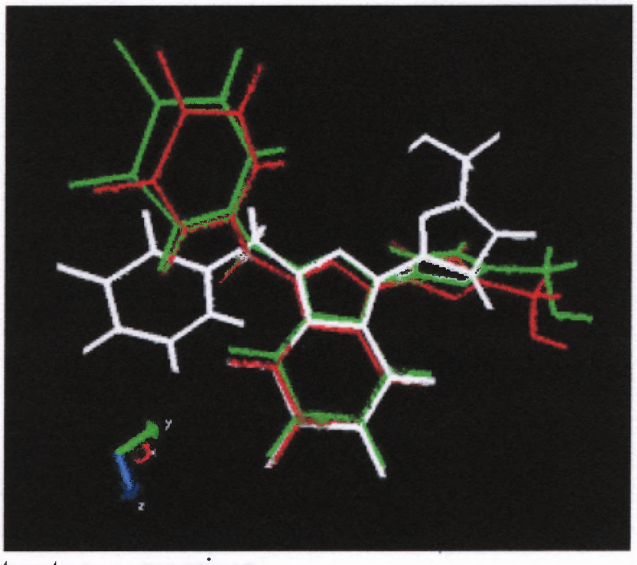

Figure 2.6 YC-1 structure comparison.

2.5 Parameter Determination of Topology File and Force Constants File

To run NAMD simulation, two parameter files must be defined. One is topology file, which contain the information of atomic mass, whole residue name, atomic charge, atom name, atom type, bond connection, double bond connection, dihedral angle, and improper. Although there are proton donor/acceptor entries, NAMD neglects that. Therefore there are no needs to define those parameters for NAMD simulation. The other is force constants parameter file, usually called simpler nomination as "parameter file", which contains force constants of bond/angle/dihedral/improper energy between each atom types, and actual bond length, angle degree. More details are available in NAMD tutorial [24].

2.5.1 Atom Type, Atomic Charge, and Group Division

Atom types were borrowed from predefined atom types. Probably some of them are good guess, and the others are not so good. However, all of atom types were defined based on very similar structure. Atomic charges were assigned based on MOPAC generated ESP

charge. Atomic residue group division was based on very similar structure in other entries.

2.5.2 Internal Coordinate

All of bond connection was edited by manually. Entry of internal coordinates ware derived from very similar structure. Each value were obtained from MOPAC output file or calculated from MOPAC output values.

2.5.3 Force Constants Parameter

As same as Section 2.2, basically all of bond length, angle, and dihedral were obtained or calculated from MOPAC output. Force constants (spring constants) were chosen from very similar structure such as benzene ring, histidine, etc. Appendix E and F are final parameter files for YC-1.

2.6 Required Parameters for Molecular Dynamics Simulation

To run molecular dynamics simulation, usually many of parameters required. Some of them are common and some of them are software suit specific. Without any doubt, one of the most important parameters in classical molecular dynamics is force field parameter. In this investigation, CHARMM force field parameters are employed. For common amino acids, DNA residue, major membrane molecule, sugar, base, and ions, public CHARMM force filed parameters are freely available from Dr. MacKerell laboratory's web site, [23]. VMD has a useful plug-in package called psfgen, which assign those CHARMM force fields to the target molecule. Other important parameters are such as time step length, total time steps, integration parameters, and temperature controls. They

were reasonably assigned. Appendix B is a sample input parameter file of MD simulation using NAMD.

2.7 Energy Minimization and Equilibrium of Base System

In NAMD tutorial [24], the procedure of typical energy minimizing and equilibrium cycle is presented. Based on the procedure, base system minimization-equilibration was conducted, so that plenty of computational time can be saved in later analysis. In the minimization process (100,000 steps), the water molecules are let move while keeping protein's configuration unchanged. Then both protein and water molecules are let move for further minimization. After this process, the system is heated gradually to room temperature using the standard protocols. After the system reaches room temperature (300K), 300ps equilibration process is performed to bring the system into an equilibrated state. Figure 2.7 is energy minimization curve of this process, and Figure 2.8 is focused area of Figure 2.7 (indicated red rectangle). It shows that around 11000 steps the base system's energy reached energy minimized state.

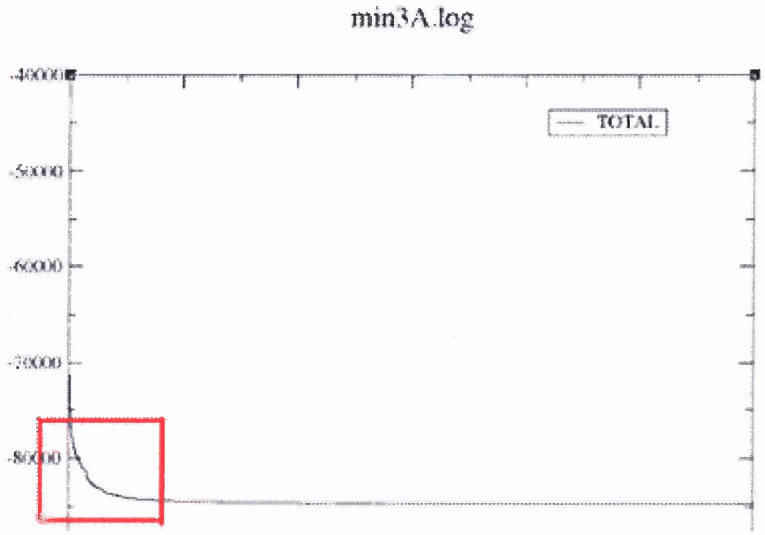

Figure 2.7 Energy minimization curve of base system.

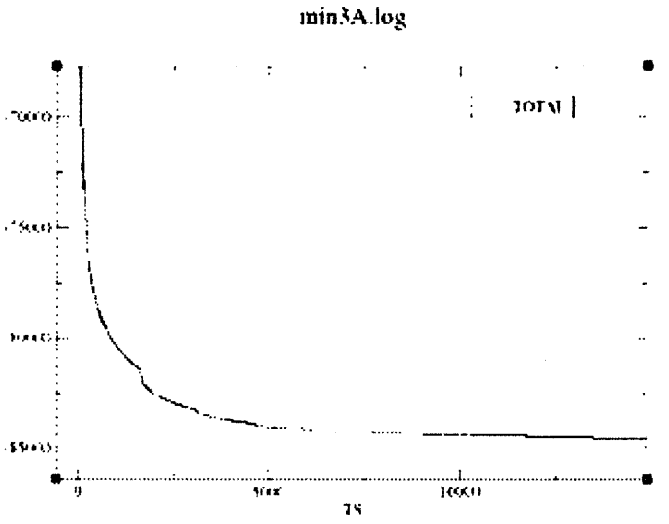

Figure 2.8 Energy minimization curve of base system (focused in).

2.8 Three Simulation Systems

Using energy minimized base system, finally three simulation systems were set up. In one system, there is no YC-1 binding. This system is called System A. In another system, YC-1 is docked such that the hydroxymethyl group is facing inside of its binding pocket (a mode termed as "Normal"). This system is called System B. The third system has YC-1 docked in the opposite orientation (a mode termed as "Flip"). Table 3.1 is a summary of each simulation system's components. Figure 2.9 shows those positions of GTP pocket and YC-1 binding pocket.

Table 2.1 Summary of Each Simulation System's Components

System Name	Components (all of components were put into 3Å thick water box)
System A	sGC, GTP, 2 Mg++ ions
System B	sGC, GTP, 2 Mg++ ions, YC-1 (Normal mode)
System C	sGC, GTP, 2 Mg++ ions, YC-1 (Flip mode)

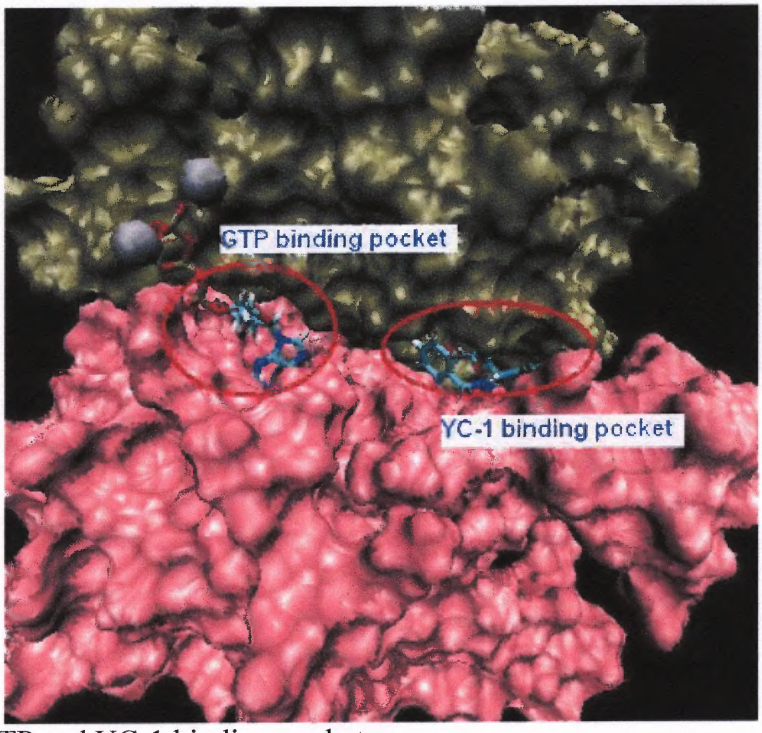

Figure 2.9 GTP and YC-1 binding pocket.

CHAPTER 3

RESULTS FROM SHORT MD SIMULATIONS

Initially, simulations of each of the three systems were conducted for 300 picoseconds. Particle Mesh Ewald (PME) [7, 38] method is used for efficient electrostatic force evaluation. Impulse multiple time stepping integration is used with inner time step of 1fs and outer time step of 3fs. The choice of these values for impulse is based on the investigation of the reference [44, 45]. The following figures (Figure 3.1, 3.2) show initial YC-1's coordinate in System B and System C.

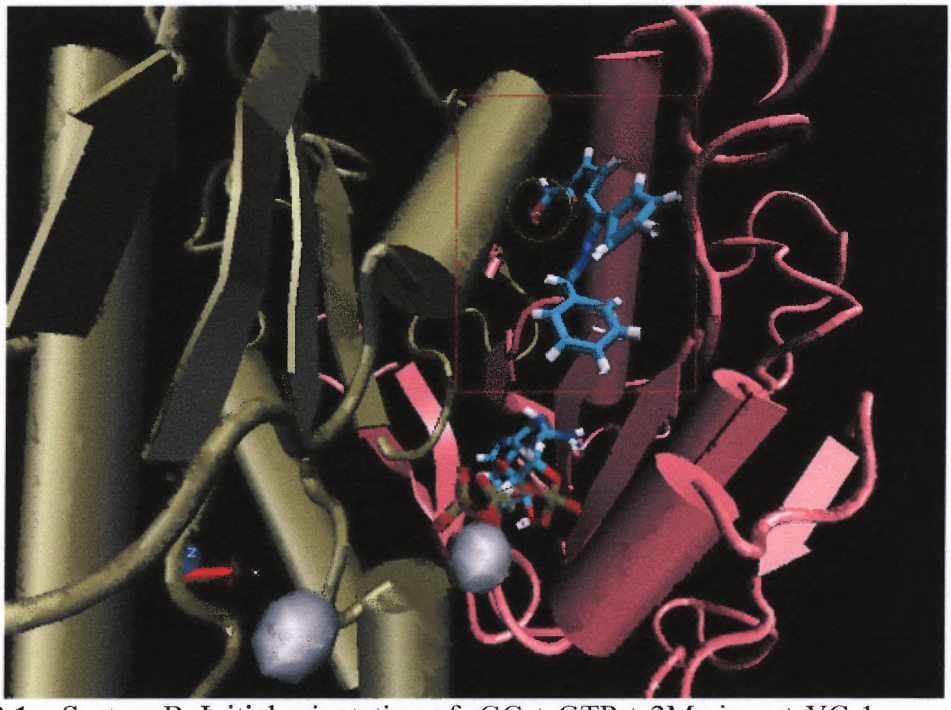

Figure 3.1 System B. Initial orientation of sGC + GTP + 2Mg ions + YC-1.

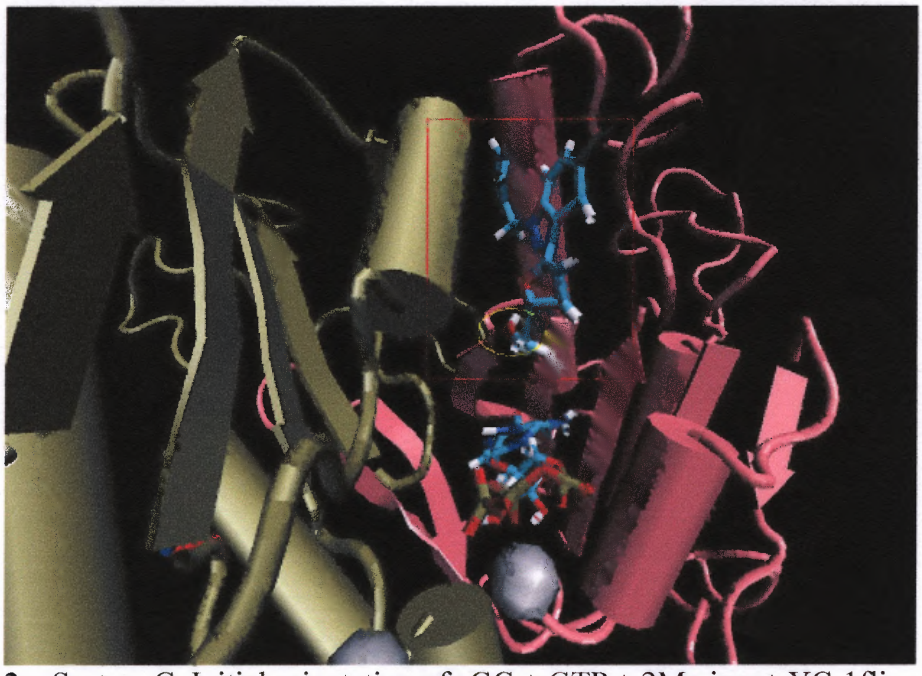

Figure 3.2 System C. Initial orientation of sGC + GTP + 2Mg ions+ YC-1flip.

3.1 YC-1's Behavior During Simulation

Figure 3.3 shows a snapshot in the simulation of System B. During the simulation the hydroxymethyl group was attracted to α_1 CYS594. Figure 3.4 shows a snapshot in the simulation of System C. During the simulation the hydroxymethyl group was attracted to α_1 CYS594 in this simulation too. Figure 3.5 is the plot of data for the distance between α_1 CYS594 and YC-1 hydroxymethyl oxygen. Block average of each 10 frames was plotted. In System B simulation, the YC-1's hydroxymethyl oxygen was constantly attracted during simulation. In System C simulation, the YC-1 hydroxymethyl oxygen repeated being attracted and bounced back, but in the end of the simulation, distance became very short. Tables 3.1 and 3.2 are numerical data. Table 3.1 refers to whole 300 picoseconds simulation, and Table 3.2 refers to last 1000 TS. Average distance shows large difference, but minimum distance is not significantly different.

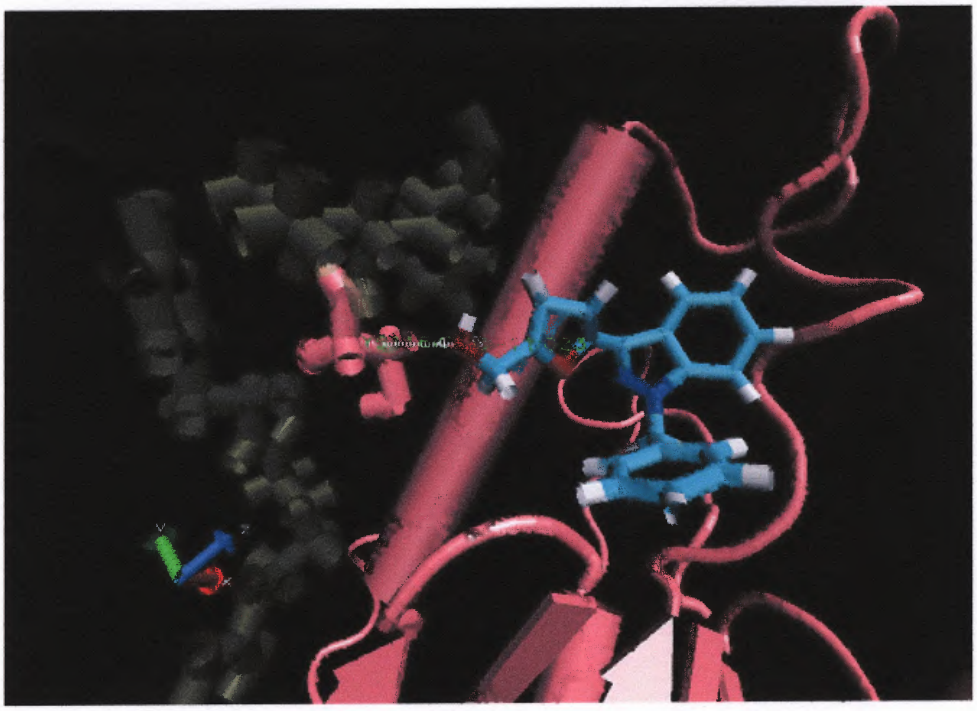

Figure 3.3 Hydroxymethyl group is attracted to α_1 CYS594 in System B.

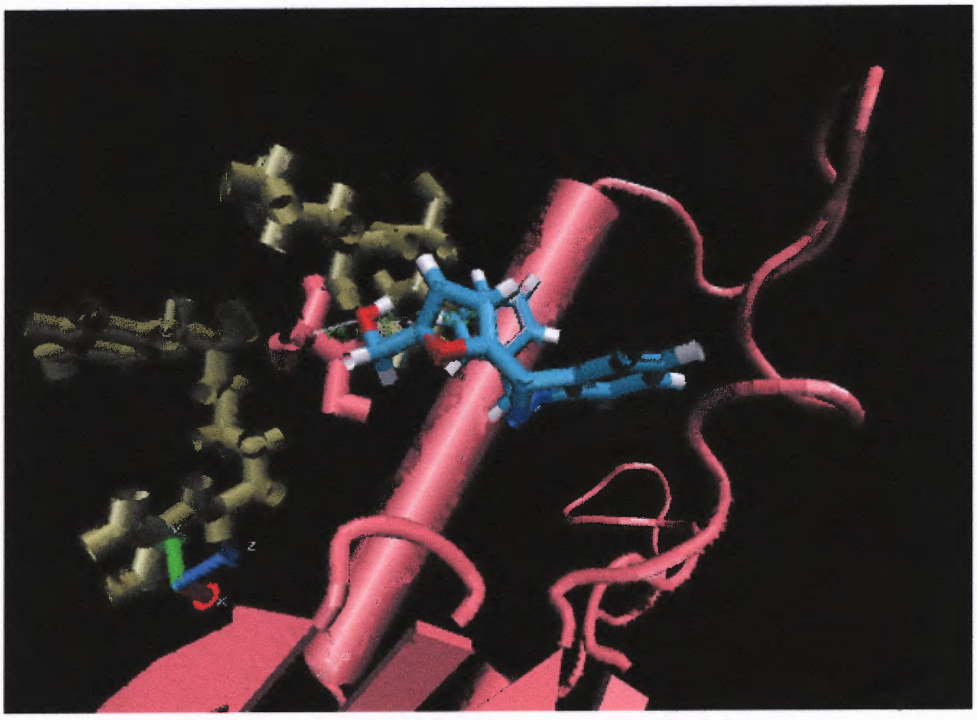

Figure 3.4 Hydroxymethyl group is attracted to α_1 CYS594 in System C.

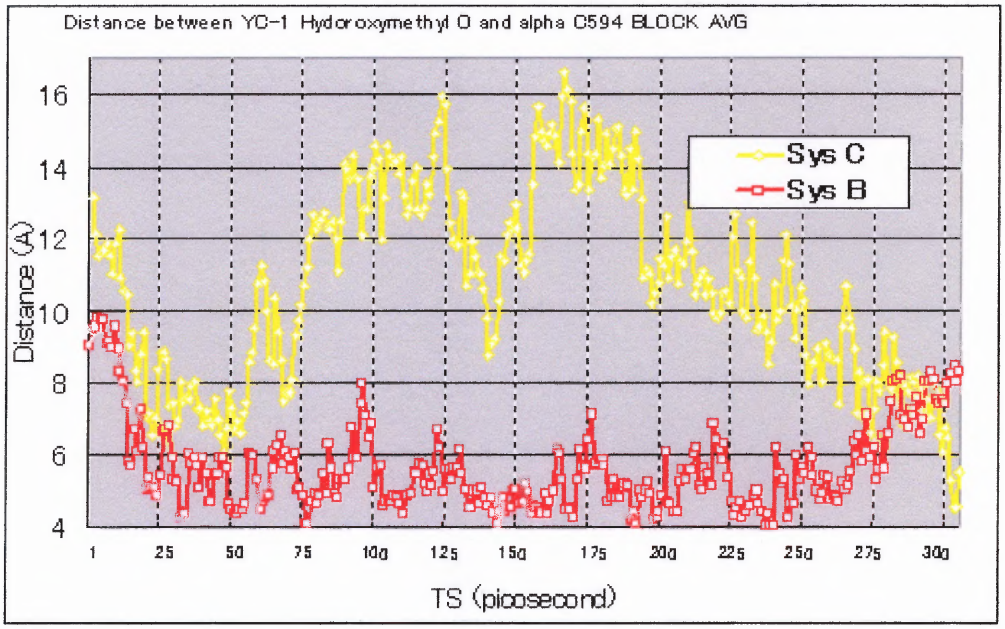

Figure 3.5 Distance between YC-1 hydroxymethyl O and α_1 CYS594.

Table 3.1 Distance Between YC-1 Hydoroxymethyl O and α_1 CYS594

300 picoseconds	System B (Å)	System C (Å)
MIN	3.359848	4.061137
MAX	9.997873	17.80521
RANGE	6.638025	13.74407
AVERAGE	5.628089	10.68674

Table 3.2 Distance Between YC-1 Hydoroxymethyl O and α_1 CYS594 of Last 1000 Time Step

Last 1000 TS	System B (Å)	System C (Å)
MIN	3.512293	4.061137
MAX	9.089073	13.51255
RANGE	5.57678	9.451414
AVERAGE	5.896177	9.06375

3.2 Three-Point Distance Change Analysis

To understand more detail, one Cα was chosen from each sGC subunit, and then distance of those three was measured. Figure 3.6 shows those three Cα's. Those are GLY528, GLY475 and SER551 in α_1, β_{1_a} and β_{1_b} subunits and chosen from near contact region of each binding pocket. Figure 3.7 shows same thing but different mode so that it can be seen those points are close to surface of the sGC.

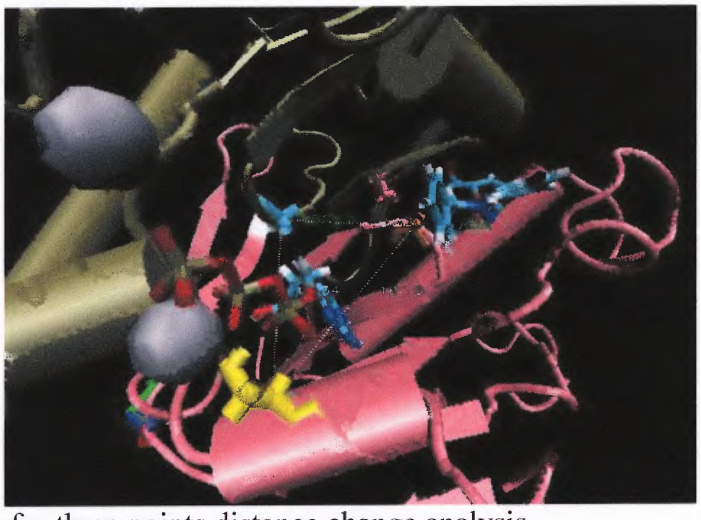

Figure 3.6 Cα's for three points distance change analysis.

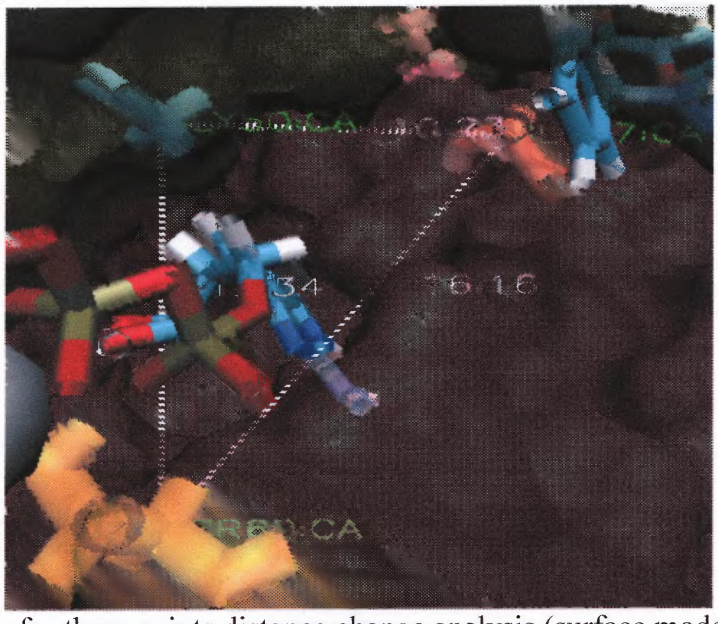

Figure 3.7 Cα's for three points distance change analysis (surface mode)

3.2.1 Distance between α_1 GLY528 and β_{1_b} GLY475

Figure 3.8 shows the distance between Cα of α_1 subunit GLY528 and β_{1_b} subunit GLY 475. Blue line shows without YC-1 simulation (System A), red line shows YC-1 normal simulation (System B), and yellow line shows YC-1 flip simulation (System C). Table 3.3 is numerical data. It seems that when YC-1 orientation is flipped, α_1 subunit and β_{1_b} subunit become slightly tight. On the other hand, when YC-1 orientation is normal, it becomes slightly loose. Difference of average between YC-1 normal and YC-1 flip simulation is about 2.6Å.

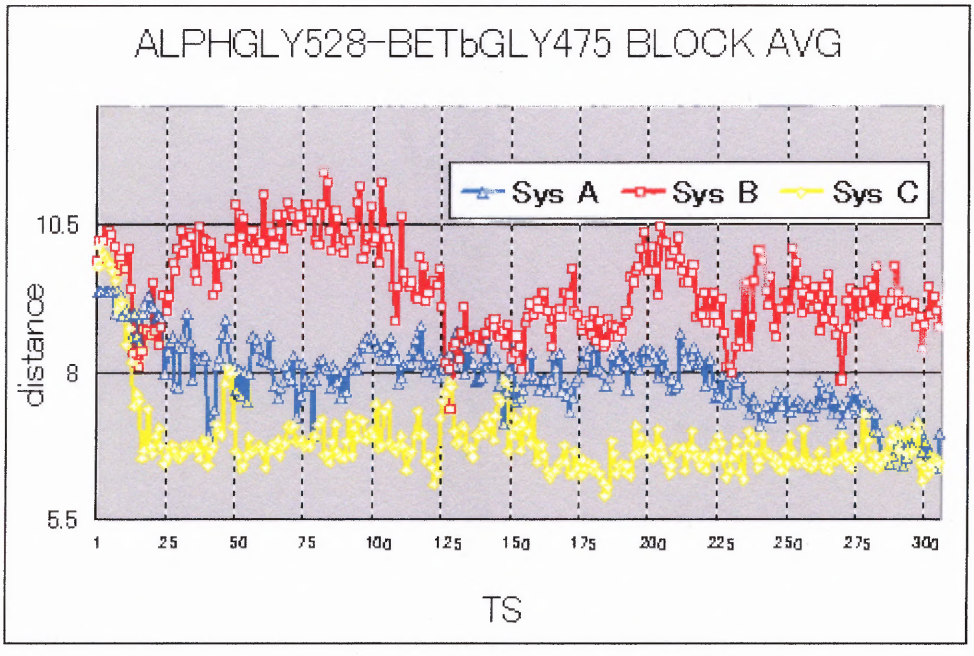

Figure 3.8 Distance between α_1 GLY528 and β_{1_b} GLY475.

Table 3.3 Distance Between α_1 GLY528 and β_{1_b} GLY475

	System A (Å)	System B (Å)	System C (Å)
MIN	5.904428	6.8032	5.495731
MAX	9.829576	11.74834	10.1269
RANGE	3.925148	4.945138	4.631169
AVERAGE	7.910935	9.434356	6.842162

3.2.2 Distance Between α_1 GLY528 and β_{1_a} SER551

Figure 3.9 shows distance between Cα of α_1 subunit GLY528 and β_{1_a} subunit SER551. Blue line shows without YC-1 simulation (System A), red line shows YC-1 normal simulation (System B), and yellow line shows YC-1 flip simulation (System C). Table 3.4 is numerical data. It seems that distance between α_1 subunit and β_{1_a} subunit was not affected from YC-1's orientation. Whether it is or even without YC-1, the distance between α_1 unit and β_{1_a} unit does not show large difference. Average distance, in the table, supports this claim.

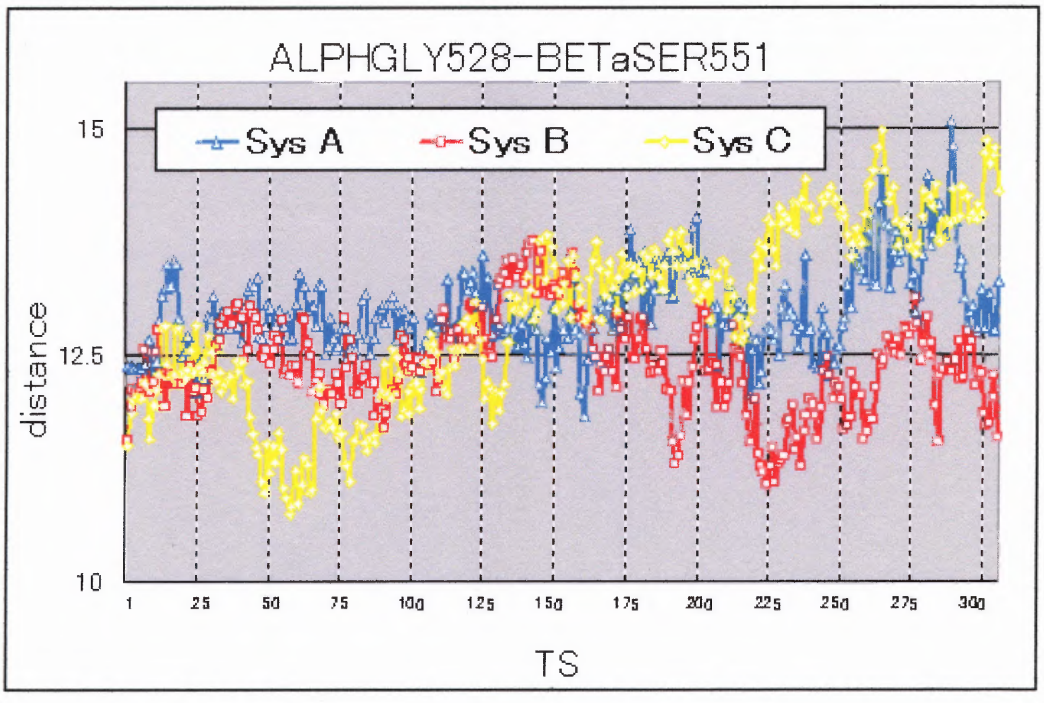

Figure 3.9 Distance between α_1 GLY528 and β_{1_a} SER551.

Table 3.4 Distance Between α_1 GLY528 and β_{1_a} SER551

	System A (Å)	System B (Å)	System C (Å)
MIN	11.3903	10.4134	10.4789
MAX	15.7422	14.2257	15.5557
RANGE	4.35199	3.81229	5.07676
AVERAGE	13.0159	12.3986	12.9531

3.2.3 Distance Between β_{1_a} SER551 and β_{1_b} GLY475

Figure 3.10 shows distance between Cα of β_{1_b} subunit GLY475 and β_{1_a} subunit SER551. Blue line shows without YC-1 simulation (System A), red line shows YC-1 normal simulation (System B), and yellow line shows YC-1 flip simulation (System C). Table 3.5 is numerical data.

Again it seems that distance between β_{1_b} subunit and β_{1_a} subunit was not affected significantly from YC-1's orientation. Whether it is or even without YC-1, the distance between β_{1_b} subunit and β_{1_a} subunit does not show large difference. Average distance, in below table, supports this claim. However, from the graph, with YC-1 normal simulation seems to make β_{1_b} and β_{1_a} a little bit tighter and with YC-1 flip simulation seems to make β_{1_b} and β_{1_a} a little bit looser. It can be bounced back again in later. Therefore perhaps more long simulation might be required.

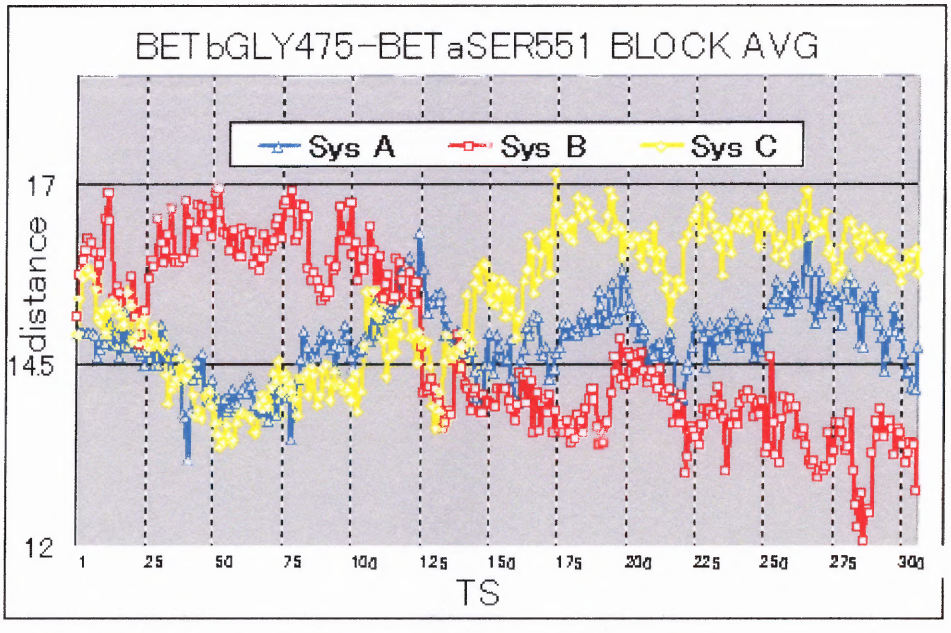

Figure 3.10 Distance between β_{1_a} SER551 and β_{1_b} GLY475.

Table 3.5 Distance Between β_{1_a} SER551 and β_{1_b} GLY475

	System A (Å)	System B (Å)	System C (Å)
MIN	12.5786	11.6017	12.7643
MAX	16.9103	17.3945	17.7511
RANGE	4.33170	5.79276	4.98678
AVERAGE	14.8362	14.7005	15.3817

3.3. Discussion from 300 Picoseconds Simulation

At this point, following intermediate hypothesis can be derived. No matter how the YC-1's orientation is, hydroxymethyl oxygen was attracted to α_1 C594, rather than Mg++ ion. It challenges the hypothesis, which was addressed in Lamothe et al. [1] partially. It seems when YC-1 orientation is flipped, α_1 subunit and β_{1_b} subunit become slightly tight. On the other hand, when YC-1 orientation is normal, it becomes slightly loose. YC-1 normal simulation (System B) seems to make β_{1_a} and β_{1_b} a little bit tighter and with YC-1 flip simulation (System C) seems to make β_{1_a} and β_{1_b} a little bit looser. Perhaps, the behavior of those molecules, especially YC-1 flipped state could be bounced back later in the time history. Therefore, longer simulation is desired.

CHAPTER 4

RESULTS FROM LONG MD SIMULATIONS

To see further details about kinetics of YC-1, GTP and sGC complex's conformational change, simulation times were expanded up to 1 nanosecond. In these simulations, one clear difference among three systems was observed in GTP's conformational change. Meanwhile, binding pocket size was also measured to obtain more detail of sGC's conformational change.

4.1 Conformational Change of GTP

4.1.1 Distance of GTP O3 and P1

When YC-1 initially binds with its System B, "Normal" orientation, GTP's conformation makes the 3' hydroxymethyl attack of the α_1 Phosphor of GTP more feasible. Figure 4.1 shows the distance between the two atoms, α_1 Phosphor P1 and 3' Oxygen O3 in GTP. As Figure 4.2 shows, they are supposed to form a bond after the cyclization. The distance is kept low, hovering at around 3.6Å in the System B, "YC-1 Normal" simulation. The distance rises to and maintains at 4.9Å in the other two simulations (since 200 ps for System C, "YC-1 Flip", simulation and since 800 ps for the System A, "Without YC-1 Binding" simulation). A smaller distance makes the cyclization reaction of GTP easier to happen, which is also known as the nucleophilic attack of the α_1 Phosphor of GTP by the 3'-hydroxymethyl Oxygen of the ribose ring of GTP. This result suggests that different initial binding mode of YC-1 makes a significant difference in terms of YC-1's catalytic potent on cyclization of GTP in sGC, and initial

"YC-1 Normal" binding mode promotes the chances of cyclization. Therefore, one possible interpretation is System A's blue line shows basal catalytic activity of sGC complex, while System B's red line shows activated catalytic activity by YC-1.

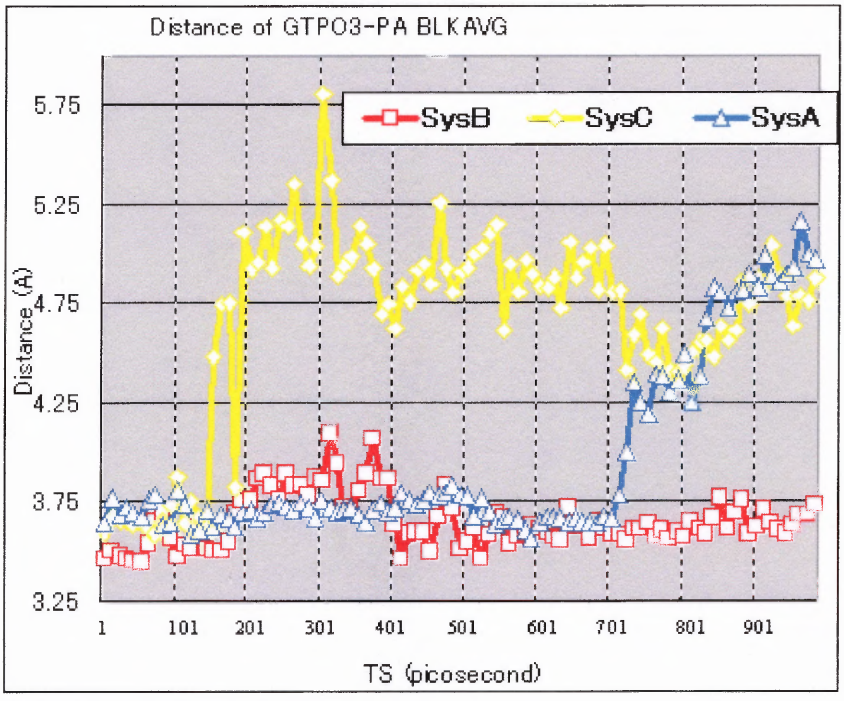

Figure 4.1 Distance of GTP O3-P1.

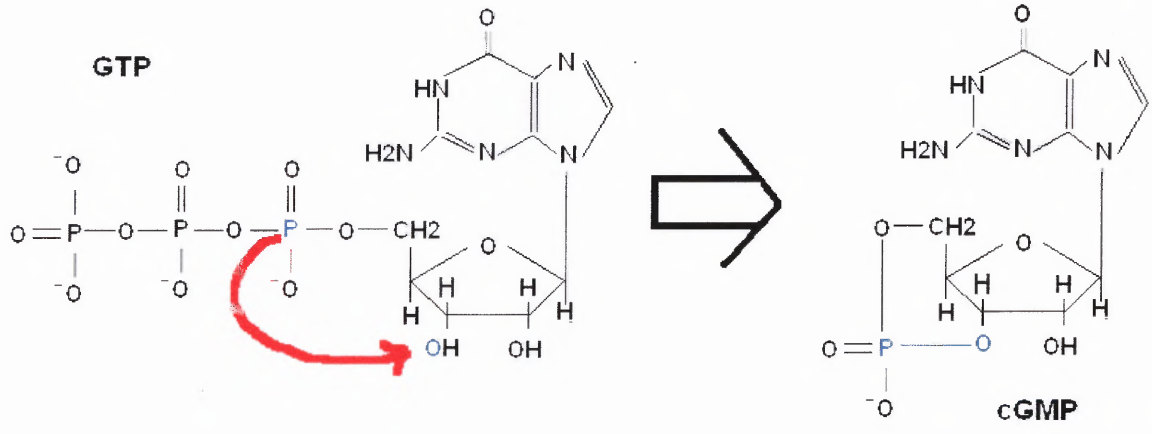

Figure 4.2 Schema of GTP to cGMP conversion.

4.1.2 YC-1 Forming Hairpin Structure

During the MD simulation, YC-1 bends to form a "hairpin" structure, as shown in Figure 4.3, inside of its binding pocket and the hydroxymethyl group does not directly interact with the GTP or magnesium ions. YC-1 does not always stay as extended in its binding pocket after initial binding as it is in vacuum. It seems that the hydroxymethyl group maintain close interaction with the Sulfur of CYS594. As shown in Figure 4.4, the distance between the Oxygen (O23) in the hydroxymethyl group and Carbon (C19) on the opposite side of YC-1 was measured through the simulations, indicating the formation of "hairpin" structure. For initial "YC-1 Normal" binding mode (System B), the YC-1 quickly forms the hairpin structure (less than 100 ps). For initial "YC-1 Flip" binding mode (System C), it takes almost 900 ps to finally reach stable hairpin structure.

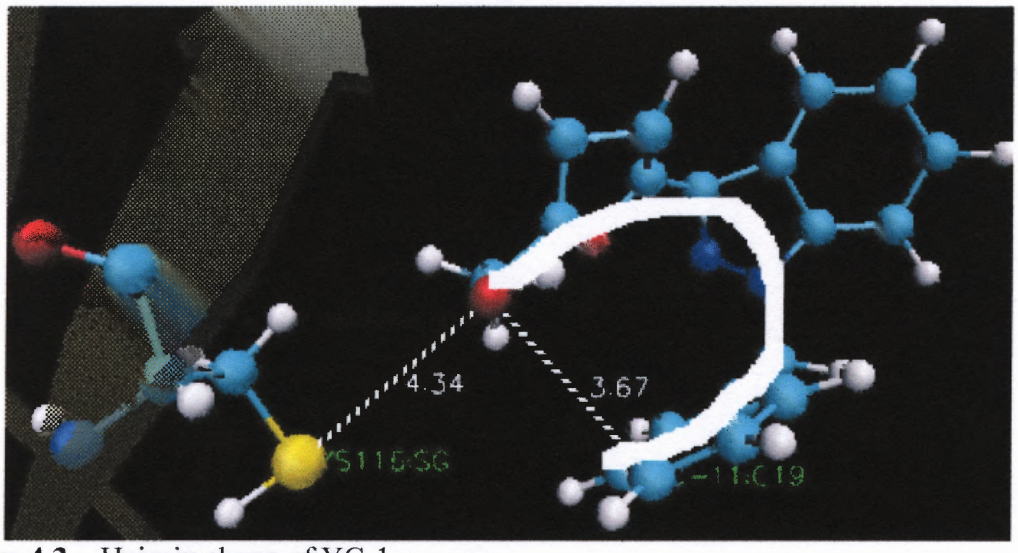

Figure 4.3 Hairpin shape of YC-1.

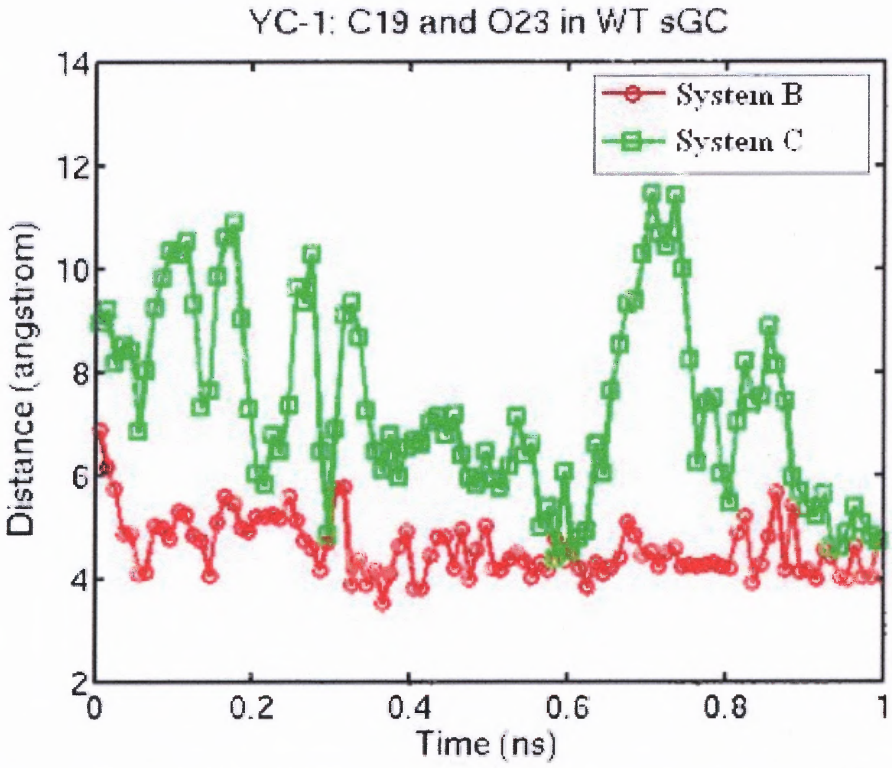

Figure 4.4 Distance plot of benzene ring and hydroxymethyl oxygen of YC-1.

4.1.3 Distance Analysis of α_1 CYS594 and YC-1's Hydroxymethyl Oxygen

Figure 4.5 shows the distance between the Oxygen (O23) in YC-1 and the Cα of α_1 CYS594. For the initial "YC-1 Flip" binding mode (System C), the hydroxymethyl "tail" of YC-1 flips back and keep close to the CYS594 residue (from 300 ps to 600 ps), bounces back again, and finally stabilizes at a close distance. The distance of the same two atoms keep fairly stable for the initial "YC-1 Normal" binding mode. Table 4.1 shows average distance of the two atoms, and it supports the claim. "YC-1 Normal" (System B) kept stable distance from early time history, while "YC-1 Flip" shows large difference in time history.

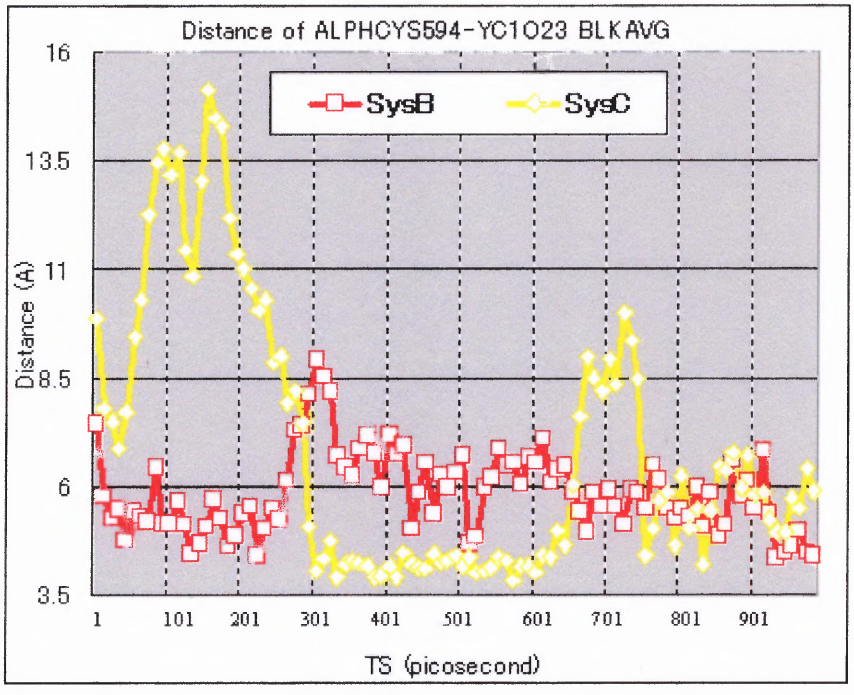

Figure 4.5 Distance of YC-1 hydroxymethyl O and α_1 CYS594 of 1ns.

Table 4.1 Average Distance of α_1 CYS594 and YC-1 Hydroxymethyl O in 300ps and 1ns Simulation

	System B (Å)	System C (Å)
300 picoseconds simulation	5.628089	10.68674
1 nanosecond simulation	5.855396	6.916178

4.1.4 Observation from Behavior of GTP and YC-1

It is observed that the "YC-1 Normal" binding mode helps YC-1 to bend to hairpin structure and stay deep inside of the binding pocket much more quickly than the "YC-1 Flip" binding mode (Figure 4.4, and 4.5). It is then postulated that this difference in the folding dynamics would result in different conformational changes in the active sites (see the following section and Appendix G), which then either promotes the chances of cyclization for the "YC-1 Normal" binding mode or has no obvious and sustained effect (Figure 4.1).

4.2 Binding Pocket Size Analysis

As same as 300 picoseconds simulation, distance between the Cα from each sub-units were measured. To obtain furthermore detail about sGC's conformation change, both YC-1 binding pocket size and GTP binding pocket size were also measured. The Cα of contact region were carefully chosen. For YC-1 pocket, front region of the pocket and deep region near to the α_1 CYS594, which attracts YC-1's hydroxymethyl oxygen, were measured. Appendix G is the detail of this analysis. From the pocket size analysis, following statements can be derived. One of the most interesting point is, System A and System B show similar tendency, while System C shows opposite tendency in many points. This observation seems to correlate with the observation of Section 4.1.4. As GTP's O3-P1 distance kept closely both in System A and System B, both system's conformational trend is same, while System C's GTP O3-P1 distance did not kept closely, System C's trend is also different from other two. As mentioned, distance of GTP O3-P1 is related with YC-1's folding dynamics, and the difference in the folding dynamics would result in different conformational changes in the active sites.

CHAPTER 5

CONCLUSIONS AND DISCUSSIONS

5.1 Conclusions

First, this work showed new hypothesis about the relation between sGC's catalytic activity and GTP, YC-1's conformational change. From Section 4.1.4, "YC-1 Normal" binding mode helps YC-1 to bend to hairpin structure and stay deep inside of the binding pocket much more quickly than the "YC-1 Flip" binding mode, then this difference in the folding dynamics would result in different conformational changes in the active sites, which then either promotes the chances of GTP cyclization for the "YC-1 Normal" binding mode or has no obvious and sustained effect. As a matter of fact, from Section 4.2, trend of pocket size change in each system seems to support this hypothesis. Secondly, this work showed strong support to Lamothe et al. [1] in terms of YC-1's catalytic activity and α_1 CYS594's relation. In this simulation, YC-1 was continuously attracted to CYS594. Third, however, this work showed partially challenge to the hypothesis of that YC-1 would be attracted Mg2+ ions in secondary binding mode. In this work, it was not really matter how the initial state of YC-1 is designed as hypothesized to be the case in Lamothe et al. [1]. In any case, YC-1 was attracted to α_1 CYS594 rather than attracted to Mg2+ ions.

5.2 Discussions

5.2.1 Atomic Charge and Optimized Structure of YC-1

It is generally accepted that ESP (Electro Static Potential), which was employed in this simulation for YC-1's parameter, is suitable for molecular dynamics simulation. For example AMBER employs ESP as its atomic charge parameter. On the other hand, CHARMM's atomic charge is derived from Mulliken charge [4, 6, 7]. This could result in that slightly difference in atomic charge distribution of YC-1, but large impact for long term molecular dynamics. Along with it, optimized structure was determined by semi empirical approach PM3 calculation in this investigation. As mentioned in Chapter 5, it is not guaranteed that semi empirical approach always generates grand energy minima state. Certainly more accurate parameter determination of YC-1 is desired. As a matter of fact, to determine those parameters require the knowledge and techniques of Computational, Quantum, and Physical Chemistry, and need to spend much time for good accuracy. Therefore determination of more accurate YC-1's parameter would be good topic for future work.

5.2 2 Solvent Size, Temperature, Pressure, Simulation Time and Other Parameters

In this simulation TIP3P water solvent model was employed and it was arranged so that water molecule makes 3Å thickness from each outmost coordinate of sGC. Where 3Å is enough thick or not can be argued. If the total volume of the simulation system is different, energy landscape, distribution might be different and affects simulation result. Same things can be said for other parameters such as temperature, pressure, and simulation time. In this investigation, PME grid model was employed and temperature was assigned every hundred time-steps so that the temperature of system keeps 300k.

However there are bunch of other simulation protocols such as constant temperature model, or constant pressure model. Different parameter setting and different combination of those parameters will affect the simulation result and perhaps there could be more realistic parameter setting. Probably, more long simulation such as 3 ns, 5 ns, or 10 ns will be more helpful to deep understanding of the systems. Add to it, simulation with thicker solvate layer would also be more robust simulation result.

5.3 Future Work

As mentioned in previous section, for future work, extending simulation time 3 to 10 ns will help to describe more detail about conformational change in later time history. Exploring with different simulation protocols, such as constant temperature, constant pressure, which close to the real biological condition, would be another good topic. Exploring different force fields to minimize force field related numerical artifacts would be challenging another topic too.

APPENDIX A

SAMPLE TCL SCRIPT FOR SOLVATION

This appendix contains tcl script cord to put your target protein into indicated thickness water layer box.

```
#please change file name and other parameters

set psffile ../pdb/sGC_Mgin.psf
set pdbfile ../pdb/sGC_Mgin.pdb
set outputname ../pdb/sGC_Mgin3AB
set thickness 3

## USAGE ##################################
#
#     Simply type in your console....
#     vmd -dispdev text -e PutInBox.tcl(or your script file name)
##########################################

package require psfgen

package require solvate

mol load psf $psffile pdb $pdbfile

#please change number into the number of A thickness you want
solvate $psffile $pdbfile -t $thickness -o $outputname

exit
```

APPENDIX B

SAMPLE NAMD CONFIGURATION

This appendix contains a sample input parameter for NAMD simulation.

```
#############################################################
## JOB DESCRIPTION                                         ##
#############################################################

# 300ps run of simulation
# sGC , 2 Mg, GTP and YC-1(flipped) in a minimized 3A Water Box.
#############################################################
## ADJUSTABLE PARAMETERS                                   ##
#############################################################

structure          ./sGCGTPYC1Flip.psf
coordinates        ./sGCGTPYC1Flip.pdb
set param_root     ../../../../TOPOandPARAMFILES
set temperature    0
set outputname     ./output/300psSim

firsttimestep      0


#############################################################
## SIMULATION PARAMETERS                                   ##
#############################################################

# Input
paraTypeCharmm      on
parameters          $param_root/par_all27_prot_na.inp
parameters          $param_root/myfile/YC1param_v3.inp
temperature         $temperature

#protocol
reassignFreq        1000
reassignTemp        25
reassignIncr                25
reassignHold        300

# Force-Field Parameters
exclude             scaled1-4
1-4scaling          1.0
cutoff              6.5
switching           on
switchdist          4.
pairlistdist        13.5
#margin              0
#pairlistdis         8.0

# Integrator Parameters
```

```
timestep            1.0  ;# 1fs/step
rigidBonds          all  ;# needed for 3fs steps
nonbondedFreq       1
fullElectFrequency  2
stepspercycle       12
#stepspercycle      16


# Constant Temperature Control
langevin            off    ;# don't do langevin dynamics
langevinDamping     5      ;# damping coefficient (gamma) of 5/ps
langevinTemp        $temperature
langevinHydrogen    off    ;# don't couple langevin bath to hydrogens

# Constant Pressure Control (variable volume)

useGroupPressure      yes ;# needed for rigidBonds
useFlexibleCell       no
useConstantArea       no

#langevinPiston       on
#langevinPistonTarget  1.01325 ;#  in bar -> 1 atm
#langevinPistonPeriod  100.
#langevinPistonDecay   50.
#langevinPistonTemp    $temperature

# Periodic Boundary Conditions

#== Min{-7.76300001144 -2.79999995232 -4.40799999237}
#== Max{56.0270004272 49.7529983521 48.4410018921}
#== Center{24.13200021 , 23.4764992 , 22.01650095 }
#== Length{ 63.79000043 , 52.5529983 , 52.84900188 }

cellBasisVector1    64.5    0.    0.
cellBasisVector2    0.    53.5    0.
cellBasisVector3    0.    0    54.
cellOrigin          24.1320    23.4765 22.0165

wrapAll             on


# PME (for full-system periodic electrostatics)
PME                 yes
PMEGridSizeX        60
PMEGridSizeY        50
PMEGridSizeZ        50


# Output
outputName          $outputname

restartfreq         500     ;# 500steps = every .5ps
dcdfreq             100     ;# 100*1= every 100fs
outputEnergies      10
outputPressure      100
```

```
xstFreq                 100
#####################################################################
## EXTRA PARAMETERS                                                ##
#####################################################################

# Spherical boundary conditions
#sphericalBC            on
#sphericalBCcenter      23.8547707501, 23.0563350236, 19.2716919904

#sphericalBCr1          32.0    #37 for big one
#sphericalBCk1          10
#sphericalBCexp1        2


#####################################################################
## EXECUTION SCRIPT                                                ##
#####################################################################

# Minimization
minimize                6000; #minimizeation 600 step
reinitvels              $temperature

run 300000 ;# 1fs * 300000 = 300 ps
```

APPENDIX C

QUICK RECIPE FOR GTP TOPOLOGY FILE

This appendix contains quick recipe for GTP topology file. The procedure is basically same as official procedure for making topology file.

1. Understand CHARMM format.
   Briefly, but well written explanation is available in NAMD tutorial's appendix [9]. Read the appendix chapter and understand it.

2. Download CHARMM parameter files.
   Publicly available CHARMM parameter file can be downloaded from following URL.
   http://www.pharmacy.umaryland.edu/faculty/amackere/force_fields.htm
   (accessed April 13. 2005).
   Unzip and untar the downloaded file. In the "stream" directory, there should be toppar_all27_na_nad_ppi.str. This file contains ATP entry (Figure C.1). Find ATP entry and cut and paste to some other text file. Along with it look inside of top_all27_prot_na.inp file, find GUA entry (Figure C.2). Cut and paste GUA entry to some other text file.

3. Merge two entries by editing carefully.
   Merge two entries by manual editing. It should be very carefully done. Following picture shows which part, from each file, should be merged (Figure C.3).

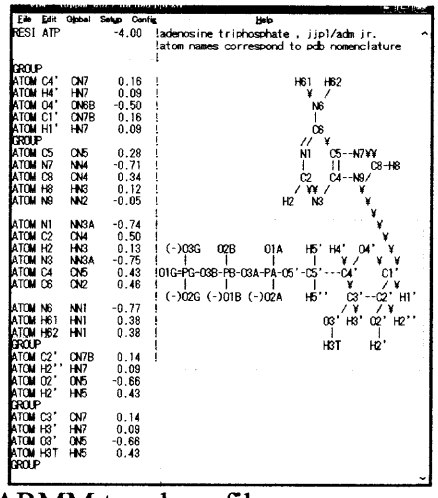

Figure C.1 ATP entry of CHARMM topology file.

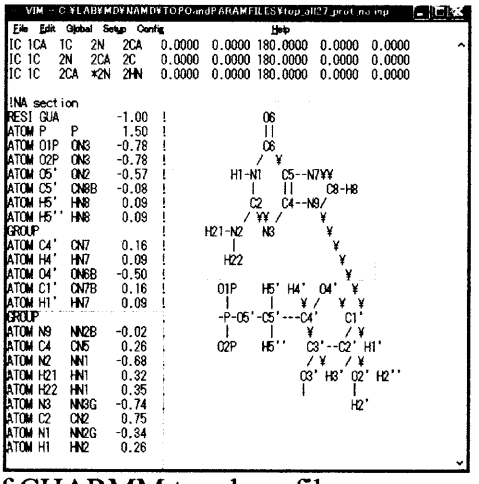

```
IC 1CA  1C   2N   2CA   0.0000  0.0000 180.0000  0.0000  0.0000
IC 1C   2N   2CA  2C    0.0000  0.0000 180.0000  0.0000  0.0000
IC 1C   2CA  *2N  2HN   0.0000  0.0000 180.0000  0.0000  0.0000

!NA section
RESI GUA          -1.00 !              O6
ATOM P    P        1.50 !              ||
ATOM O1P  ON3     -0.78 !              C6
ATOM O2P  ON3     -0.78 !             /  ¥
ATOM O5'  ON2     -0.57 !          H1-N1   C5--N7¥¥
ATOM C5'  CN8B    -0.08 !           |   ||    C8-H8
ATOM H5'  HN8      0.09 !           C2   C4--N9/
ATOM H5'' HN8      0.09 !          / ¥¥ /      ¥
GROUP                   !      H21-N2   N3      ¥
ATOM C4'  CN7      0.16 !        |                ¥
ATOM H4'  HN7      0.09 !       H22                ¥
ATOM O4'  ON6B    -0.50 !                          ¥
ATOM C1'  CN7B     0.16 !        O1P    H5' H4'  O4' ¥
ATOM H1'  HN7      0.09 !        |      |   ¥ /   ¥  ¥
GROUP                   !       -P-O5'-C5'---C4'    C1'
ATOM N9   NN2B    -0.02 !        |      |    ¥       / ¥
ATOM C4   CN5      0.26 !       O2P    H5''   C3'--C2' H1'
ATOM N2   NN1     -0.68 !                    / ¥     / ¥
ATOM H21  HN1      0.32 !                  O3' H3' O2' H2''
ATOM H22  HN1      0.35 !                  |       |
ATOM N3   NN3G    -0.74 !                         H2'
ATOM C2   CN2      0.75 !
ATOM N1   NN2G    -0.34 !
ATOM H1   HN2      0.26
```

Figure C.2 GUA entry of CHARMM topology file.

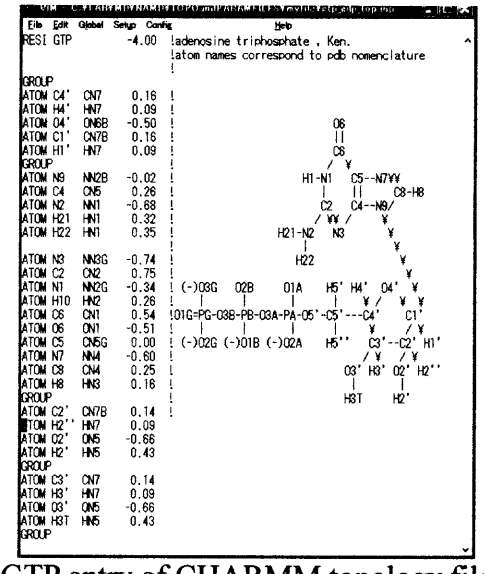

```
RESI GTP          -4.00 !adenosine triphosphate , Ken.
                        !atom names correspond to pdb nomenclature
                        !
GROUP
ATOM C4'  CN7      0.16 !
ATOM H4'  HN7      0.09 !
ATOM O4'  ON6B    -0.50 !                    O6
ATOM C1'  CN7B     0.16 !                    ||
ATOM H1'  HN7      0.09 !                    C6
GROUP                   !                   /  ¥
ATOM N9   NN2B    -0.02 !                H1-N1   C5--N7¥¥
ATOM C4   CN5      0.26 !                 |   ||    C8-H8
ATOM N2   NN1     -0.68 !                 C2   C4--N9/
ATOM H21  HN1      0.32 !                / ¥¥ /      ¥
ATOM H22  HN1      0.35 !           H21-N2   N3      ¥
                        !            |               ¥
ATOM N3   NN3G    -0.74 !           H22               ¥
ATOM C2   CN2      0.75 !                             ¥
ATOM N1   NN2G    -0.34 ! (-)O3G   O2B     O1A    H5' H4'  O4'  ¥
ATOM H10  HN2      0.26 !  |       |       |      |   ¥ /   ¥  ¥
ATOM C6   CN1      0.54 !O1G=PG-O3B-PB-O3A-PA-O5'-C5'---C4'    C1'
ATOM O6   ON1     -0.51 !  |       |       |      |    ¥       / ¥
ATOM C5   CN5G     0.00 ! (-)O2G (-)O1B (-)O2A    H5''   C3'--C2' H1'
ATOM N7   NN4     -0.60 !                              / ¥    / ¥
ATOM C8   CN4      0.25 !                           O3' H3' O2' H2''
ATOM H8   HN3      0.16 !                           |       |
GROUP                   !                          H3T     H2'
ATOM C2'  CN7B     0.14 !
ATOM H2'' HN7      0.09
ATOM O2'  ON5     -0.66
ATOM H2'  HN5      0.43
GROUP
ATOM C3'  CN7      0.14
ATOM H3'  HN7      0.09
ATOM O3'  ON5     -0.66
ATOM H3T  HN5      0.43
GROUP
```

Figure C.3 Hand made GTP entry of CHARMM topology file.

APPENDIX D

Z-MATRIX DERIVED FROM COLLABORATOR'S WORK

This appendix contains z-matrix derived from initial YC-1 coordinates.

pm3 precise thermo(298,1498,100) rot =5 esp
Zmatrix of YC-1 generated by Insight2 and molden

atom	bond length	angle	dihedral	connections		
C	0.000000 0	0.000000 0	0.000000 0	0	0	0
C	1.398366 1	0.000000 0	0.000000 0	1	0	0
C	1.388535 1	122.304619 1	0.000000 0	2	1	0
C	1.404024 1	119.200371 1	0.483359 1	3	2	1
C	1.401747 1	119.202919 1	0.776557 1	4	3	2
C	1.401115 1	120.735992 1	-0.854586 1	5	4	3
N	1.376559 1	106.409332 1	179.939621 1	2	3	4
N	1.349442 1	109.537590 1	-0.989273 1	7	2	3
C	1.327118 1	108.748215 1	-0.286042 1	8	7	2
C	1.470606 1	111.001938 1	173.180099 1	7	8	9
C	1.521322 1	111.493828 1	161.347809 1	10	7	8
C	1.400327 1	122.781723 1	140.510910 1	11	10	7
C	1.396597 1	122.118324 1	-176.628586 1	12	11	10
C	1.392641 1	119.720940 1	0.291434 1	13	12	11
C	1.391134 1	119.629982 1	-2.295671 1	14	13	12
C	1.396589 1	119.741898 1	0.703137 1	15	14	13
C	1.486132 1	112.927116 1	-175.006134 1	9	8	7
C	1.334077 1	129.502029 1	179.444901 1	17	9	8
C	1.463955 1	104.541809 1	-175.480209 1	18	17	9
C	1.345915 1	104.751884 1	-1.459649 1	19	18	17
O	1.274183 1	108.439018 1	0.254387 1	20	19	18
C	1.520073 1	130.167343 1	179.352005 1	20	19	18
O	1.442418 1	110.156258 1	-172.125122 1	22	20	19
H	1.067135 1	119.938423 1	-176.011612 1	12	11	16
H	1.080447 1	120.319824 1	-179.717590 1	13	12	11
H	1.074717 1	120.090797 1	178.588058 1	14	13	12
H	1.077435 1	119.843506 1	-179.626602 1	15	14	13
H	1.074361 1	119.215668 1	177.396194 1	16	11	12
H	1.103726 1	111.951866 1	19.397820 1	10	11	12
H	1.109308 1	108.963600 1	-98.085014 1	10	11	12
H	1.074149 1	132.258957 1	2.761100 1	18	17	9
H	1.077266 1	123.918610 1	177.514465 1	19	18	17
H	1.108878 1	110.399071 1	65.678558 1	22	20	19
H	1.113746 1	109.276886 1	-50.763268 1	22	20	19
H	0.980058 1	99.903328 1	15.133488 1	23	22	20
H	1.074014 1	120.005440 1	-2.464082 1	4	3	9
H	1.078237 1	119.871223 1	179.235046 1	5	4	3
H	1.080243 1	120.409615 1	179.476410 1	6	5	4
H	1.079063 1	121.928581 1	-1.555466 1	1	2	7

APPENDIX E

YC-1 TOPOLOGY FILE

This appendix contains topology entry of YC-1 in CHARMM format.

```
¥¥¥¥ CHARMM28 All-Hydrogen Nucleic Acid Topology File ////
*  ¥¥¥¥¥¥¥¥¥¥¥¥¥¥¥¥¥¥ Developmental //////////////////////
* TRIAL FOR YC-1 topology
27 1

!
DEFA FIRS none LAST none
AUTOGENERATE ANGLES DIHEDRALS
RESI YC-1          0.0000 !
GROUP                     !
ATOM C19  CA      -0.0906 !
ATOM H26  HP       0.1021 !
GROUP                     !
ATOM C20  CA      -0.1027 !
ATOM H27  HP       0.1073 !
GROUP                     !
ATOM C21  CA      -0.0846 !
ATOM H28  HP       0.1038 !
GROUP                     !
ATOM C18  CA      -0.1021 !
ATOM H25  HP       0.1086 !
GROUP                     !
ATOM C17  CA      -0.0724 !
ATOM H24  HP       0.1173 !
GROUP                     !
ATOM C16  CA      -0.1250 !
GROUP                     !
ATOM C15  CT2     -0.0118 !
ATOM H29  HA       0.0858 !
ATOM H30  HA       0.0675 !
                          !
GROUP                     !
ATOM C9   CPT     -0.1428 !
ATOM N8   NY       0.2495 !
ATOM N7   NY      -0.1684 !
ATOM C6   CY      -0.0157 !
ATOM C10  CPT     -0.1194 !
GROUP                     !
ATOM C11  CA      -0.0264 !
ATOM H34  HP       0.1158 !
```

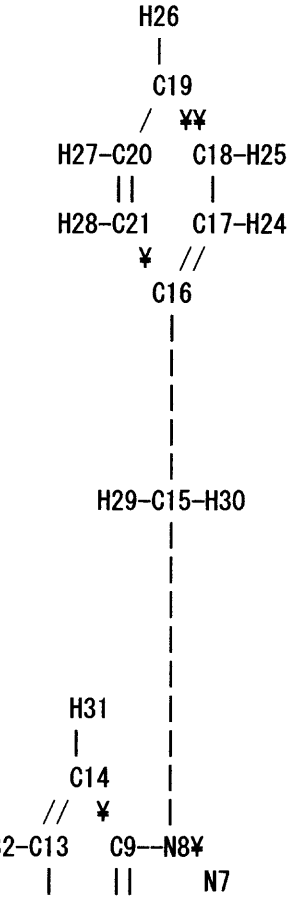

```
GROUP                    !          C12   C10-C6//
ATOM C12  CA     -0.1334 !         / ¥¥ /      |
ATOM H33  HP      0.1083 !       H33  C11      |
GROUP                    !             |      |
ATOM C13  CA     -0.0689 !            H34     |
ATOM H32  HP      0.0989 !                     |
GROUP                    !                    |
ATOM C14  CA     -0.1093 !                    |
ATOM H31  HP      0.1102 !                    |
                         !                    |
GROUP                    !                    |
ATOM O2   O      -0.0475 !                    |
ATOM C1   CPH1   -0.0663 !                    |
ATOM C22  CT2     0.1509 !                    |
ATOM H37  HA      0.0336 !  H39   H37    O2---C3
ATOM H38  HA      0.0323 !    ¥    |    /     ||
GROUP                    !    O23-C22-C1      ||
ATOM C3   CPH2    0.0368 !         |   ¥¥     ||
ATOM C4   CPH2   -0.1454 !        H38   C5----C4
ATOM H35  HR1     0.1362 !               |     |
ATOM C5   CPH1   -0.1509 !              H36   H35
ATOM H36  HR3     0.1344 !
GROUP                    !
ATOM O23  OH1    -0.3018 !
ATOM H39  H       0.1861 !
BOND H26  C19  C19  C20  C20  H27  C21  H28  C21  C16  C17  H24  C17  C18  H25  C18
BOND C15  C16  C15  H29  C15  H30
BOND N8   C15  N8   N7   N8   C9   C9   C14  C14  H31  C13  H32  C13  C12
BOND C12  H33  C11  H34  C11  C10  C10  C6
BOND C6   C3   C3   O2   O2   C1   C1   C22  C22  H37  C22  H38  C5   H36  C4   H35
BOND C22  O23  O23  H39  C4   C5
DOUBLE  C20  C21  C16  C17  C18  C19
DOUBLE  C9   C10  C13  C14  C11  C12  C6   N7
DOUBLE  C3   C4   C1   C5

!DONOR HN N
!ACCEPTOR O C

!IMPR N -C CA HN  C CA +N O

IMPR  N7   C6   C10  C9   ! 1.3562  106.89   -0.18  106.74  1.4082

!IC AT1  AT2  AT3  AT4   BOND-L  ANGLE    DIHED     ANGLE    BOND-L
!                        AT1:AT2 1:2:3    1:2:3:4   2:3:4     3:4
!
!IC AT1  AT2  *A3  AT4   BOND-L  ANGLE    DIHED     ANGLE    BOND-L
!                        AT1:AT3 1:3:2    1:2:3:4   2:3:4     3:4
!IC -C   CA   *N   HN    1.3551 126.4900  180.0000 115.4200  0.9996
```

```
IC  C20  C19  C18  C17   1.4026  121.82   -0.32  119.19   1.3900 ! All geometory was
generated by MOPAC6
IC  C18  C19  C20  C21    1.3985  121.82    0.32  119.13   1.3863 ! PM3 PRECISE
calculation
IC  C19  C18  C17  C16   1.3985  119.19    0.37  120.13   1.3915 !
IC  C21  C17  *C16  C15  1.3915  120.43  179.72  119.97   1.500 !
IC  C18  C20  *C19  H26  1.3985  120.82  179.42  119.93   1.0951 !
IC  C17  C19  *C18  H25  1.3900  119.19  179.97  120.31   1.0938 !
IC  C21  C19  *C20  H27  1.3863  119.13  179.96  120.26   1.0948 !
IC  C16  C18  *C17  H24  1.3915  120.13  179.55  119.98   1.0971 !
IC  C16  C20  *C21  H28  1.3915  120.28  179.25  119.59   1.0969 !
IC  C17  C16  C15  N8    1.3915  119.97   78.13  112.51   1.4789 !
IC  N8   C16  *C15  H30  1.4789  112.51  120.31  110.46   1.1101 !
IC  H30  C16  *C15  H29  1.1101  110.46 -121.84  109.87   1.1095 !

IC  C6   N7   N8   C9    1.3562  110.17    0.98  109.60   1.3992
IC  C10  C3   *C6  N7    1.4530  130.57 -179.59  122.55   1.3562
IC  C10  C6   N7   N8    1.4530  106.89   -0.49  110.16   1.3586
IC  C9   C6   *C10 C11   1.4082  106.74  179.21  133.69   1.3965
IC  C9   C10  C11  C12   1.4082  119.54    0.55  119.58   1.3722
IC  C10  C11  C12  C13   1.3965  119.58   -0.60  119.78   1.4215
IC  C11  C12  C13  C14   1.3721  119.78    0.46  121.82   1.3730
IC  C12  C10  *C11 H34   1.3721  119.58  179.74  118.22   1.0965
IC  C13  C11  *C12 H33   1.4215  119.78  179.88  120.25   1.0939
IC  C14  C12  *C13 H32   1.3730  121.82  179.86  118.49   1.0947
IC  C9   C13  *C14 H31   1.3921  117.62 -179.51  121.83   1.0971
IC  N7   C9   *N8  H15   1.3586  109.60 -175.09  127.17   1.4789
IC  N7   C10  *C6  C3    1.3562  106.89 -179.64  130.57   1.4406

IC  C22  C1   O2   C3    1.4918  118.20  179.53  105.68   1.3962
IC  C1   O2   C3   C4    1.3882  105.68    0.14  109.73   1.3709
IC  O2   C3   C4   C5    1.3962  109.73   -0.34  108.06   1.4309
IC  C3   C4   C5   C1    1.3709  108.06    0.34  105.29   1.3813
IC  C4   C5   C1   O2    1.4309  105.29   -0.26  111.27   1.3882
IC  C5   C1   O2   C3    1.3813  111.27    0.09  105.68   1.3962
IC  C5   C4   C3   C6    1.4309  108.37  187.57  132.15   1.4406
IC  C22  C1   C5   H36   1.4918  130.53    0.69  127.25   1.0851
IC  C5   C1   C22  H37   1.3813  130.53  138.97  110.66   1.1087
IC  C5   C1   C22  H38   1.3313  130.53   20.62  108.93   1.1085
IC  C5   C1   C22  O23   1.3313  130.53  -99.15  108.02   1.4098
IC  C1   C22  O23  H39   1.4918  108.02 -174.02  107.00   0.9471
IC  C5   C3   *C4  H35   1.4309  108.06 -179.52  126.51   1.0879

!IC  C4   C5   C1    HG   *1.3165 *108.68  *172.86 *131.52 *1.5421
!IC   C1    C22    O23    $$HA2    0.0       0.0    -60.0     0.0    0.0
!IC   C1    C22    O23    $$HA3    0.0       0.0     60.0     0.0    0.0
!IC  C4   C3   O2   $$HD1    1.3071  110.31  157.04  123.39   0.9770
```

APPENDIX F

YC-1 CONSTANTS PARAMETER FILE

This appendix contains force constants parameter entry of YC-1 in CHARMM format.

```
BONDS
!
!V(bond) = Kb(b - b0)**2
!!
!Kb: kcal/mole/A**2 (spring constats)
!b0: A (bond length)
! 4.34E-02
! spring constants is usually around 6.5 eV/Angstrome(bond length)^2
!   C      C        600.000         1.3350 ! ALLOW ARO HEM
!                      ! Heme vinyl substituent (KK, from propene (JCS))
!   CA     CA      305.000         1.3750 ! ALLOW     ARO
!                      ! benzene, JES 8/25/89


!atom type Kb              b0
!

CPH2 CPH2   350.000         1.3718 ! Spring constant is guess!!
                    !
CPH2 CY     220.000         1.4390 ! Spring constant is guess!!
                    !
O      CPH1   240.000         1.3880 ! Spring constant is guess!!
                    !
O      CPH2   260.000         1.3961 ! Spring constant is guess!!
                    !
CPH1 CPH2   220.000         1.4304 ! Spring constant is guess!
                    ! Spring constant is guess!!
NY     CT2    222.500         1.4791 ! DUMMY
                    ! Spring constant is guess!!
NY     CY     358.000         1.3550 ! DUMMY
                    ! Spring constant is guess!!
NY     NY     270.000         1.3583 !DUMMY
                    ! Spring constant is guess!!

ANGLES
!
!V(angle) = Ktheta(Theta - Theta0)**2
!
!V(Urey-Bradley) = Kub(S - S0)**2
!
!Ktheta: kcal/mole/rad**2
!Theta0: degrees
!Kub: kcal/mole/A**2 (Urey-Bradley)
!S0: A
!
```

```
!atom types        Ktheta      Theta0     Kub        S0!example
!OS     CD     CT3     55.000       109.00     20.00     2.32600 ! ALLOW POL PEP
                     ! adm jr., 4/05/91, for PRES CT1 from methylacetate
!OM     FE     NPH         5.000       90.0000 ! ALLOW HEM
                     ! Heme (6-liganded): ligand links (KK 05/13/91)

!@@@@@All of spring constants are guessed from CHARMM22,27 similer structure.@@@
!@@@@@All of angles were obtained from the result of PM3 calculation.@@@

CPT   NY    NY      120.000   109.638 !
CY    NY    NY      100.000   110.156 !
CPH2 CPH2 CY      110.000   132.154 !
CPH2 CPH2 O       110.000   109.708 !
CPH2 CPH2 HR1      25.000   126.470 !
CPH2 CY    NY      45.000   122.540 !
CPH1 CPH1 O       45.000   130.531 !
CPH1 O      CPH2  130.000   105.709 !
CPH1 CT2   OH1     58.385   107.995 !
CY    CPH2 O      112.000   118.138 !
CPT   CY    NY      45.000   122.540 !
CPH2 CY    CPT     45.000   130.157 !
CPH1 CPH1 CPH2  130.000   105.287 !
CPH1 CPH2 CPH2  130.000   108.026 !
CPH1 CPH2 HR1      25.000   125.503 !
CPH2 CPH1 HR3      25.000   127.461 !
CT2   CPH1 O       45.800   118.196 !
HA    CT2   NY      33.430   109.500 !
CT2   NY    NY      45.800   130.000 !
CPT   NY    CT2     45.800   127.123 !
CA    CT2   NY      51.800   112.523 !

DIHEDRALS
!
!V(dihedral) = Kchi(1 + cos(n(chi) - delta))
!
!Kchi: kcal/mole
!n: multiplicity
!delta: degrees
!
!atom types                Kchi      n     delta
!


!@@@@@@@@@DUMMYS@@@@@@@@@@@@@@@@@@@@@@@@

CA     CT2    NY     NY     0.160 1    -92.178 !
CA     CT2    NY     CPT    0.000 1     81.765 !
CT2    NY     NY     CY     0.800 2    176.326 ! !
CT2    NY     CPT    CA     0.800 2      5.734 ! !
CT2    NY     CPT    CPT    0.800 2   -176.165 ! !
HA     CT2    NY     NY     0.250 2    145.344 !
HA     CT2    NY     CPT    0.250 2    -40.172 !
CPT    CPT    CY     CPH2   1.500 2   -179.820 !
NY     NY     CY     CPH2   1.500 2    179.185 !
NY     CY     CPH2   O      1.400 1    155.684 !
NY     CY     CPH2   CPH2   0.000 3    -21.109 !
```

```
CY      CPH2  O     CPH1   0.000 3   -178.917 !
CY      CPH2  CPH2  HR1    0.000 3      0.915 !
CY      CPH2  CPH2  CPH1   3.000 2    178.574 !
CPT     CY    CPH2  O      1.100 1    -24.729 !
CPT     CY    CPH2  CPH2   0.000 3    156.477 !
CA      CPT   CY    CPH2  11.000 2     -0.162 !
O       CPH2  CPH2  HR1    3.000 2   -179.821 !
O       CPH1  CT2   HA     0.190 2    -40.333 !
O       CPH1  CT2   OH1    0.190 1     81.544 !
O       CPH1  CPH1  HR3    3.000 2   -179.969 !
CPH1    CPH1  CPH2  HR1    3.000 2    179.968 !
CT2     CPH1  O     CPH2   3.000 2    179.521 !
CT2     CPH1  CPH1  CPH2   3.000 2   -179.604 !
CPH2    CPH2  CPH1  HR3    3.000 2   -179.957 !
HR1     CPH2  CPH1  HR3    1.000 2     -0.426 !
CPH1    CPH1  CT2   OH1    0.200 1    -99.153 !


CPT     NY    NY    CY    16.000 2      0.991 !
NY      NY    CY    CPT    6.000 2     -0.487 !
NY      CY    CPT   CA     1.500 2    179.024 !
NY      NY    CPT   CA     2.000 2   -179.167 !
NY      NY    CPT   CPT   16.000 2     -1.076 !
O       CPH2  CPH2  CPH1  14.000 2     -0.296 !
O       CPH1  CPH1  CPH2  14.000 2     -0.263 !
CPH1    CPH1  CPH2  CPH2  14.000 2      0.338 !
CPH1    O     CPH2  CPH2  14.000 2      0.133 !
CPH2    O     CPH1  CPH1  14.000 2      00.089 !

CPT     CPT   CY    NY     6.000 2     -0.184 !

IMPROPER
!
!V(improper) = Kpsi(psi - psi0)**2
!
!Kpsi: kcal/mole/rad**2
!psi0: degrees
!note that the second column of numbers (0) is ignored
!
!atom types             Kpsi                   psi0
!

CPT     CPT   CY    NY     6.000 2     -0.184 !

END
```

APPENDIX G

DETAIL OF BINDING POCKET ANALYSIS

This appendix contains the detail of binding pocket analysis in 1 ns simulation. Figures G1 to G.3 show three points analysis plot data. Tables G1 to G.3 show comparison of average distance between 300 ps simulation and 1ns simulation. Figure G.4 shows selected points of front end of YC-1 binding pocket. Figure G.5 shows its side view. From Figures G.6 to G.9 shows distance plot data of them. Figure G.10 shows selected points of deep inside of YC-1 binding pocket. Figures G.11 and G.12 show distance plot of them. Figures G.13, G.14, and G.15 show that GTP pocket is knapsack-like structure. Figures G.16, G.17 and G.18 show distance plot of selected points.

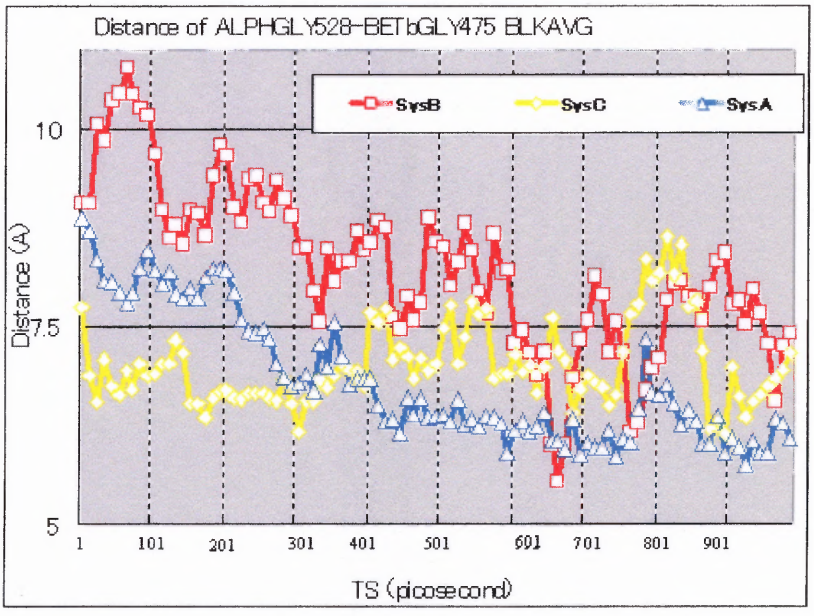

Figure G.1 Distance of α_1 GLY528 and β_{1_b} GLY475 in 1ns simulation

Table G.1 Distance Between α_1 GLY528 and β_{1_b} GLY475 in 1ns Simulation

	System A (Å)	System B (Å)	System C (Å)
300 ps simulation	7.910935	9.434356	6.842162
1 ns simulation	6.835958	8.238168	7.025485

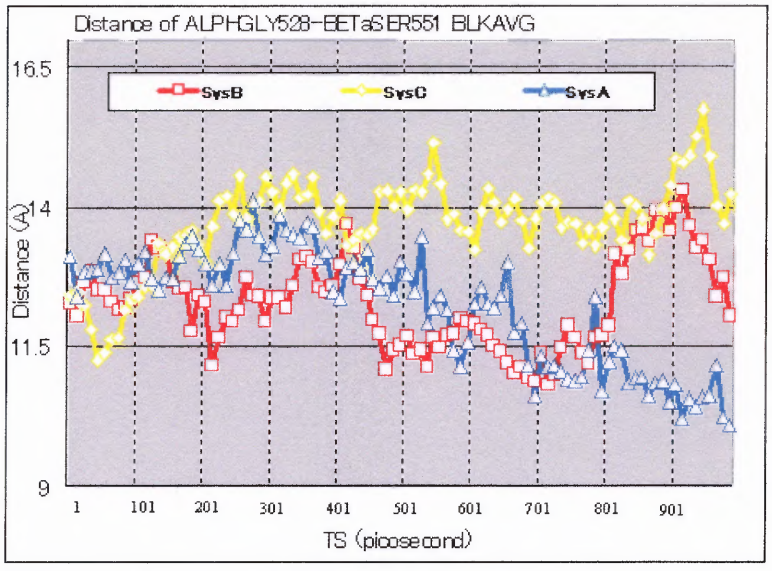

Figure G.2 Distance of α_1 GLY528 and β_{1_a} SER551 in 1ns simulation.

Table G.2 Distance Between α_1 GLY528 and β_{1_a} SER551 in 1ns simulation

	System A (Å)	System B (Å)	System C (Å)
300 ps simulation	13.0159	12.3986	12.9531
1 ns simulation	12.22774	12.29142	13.71343

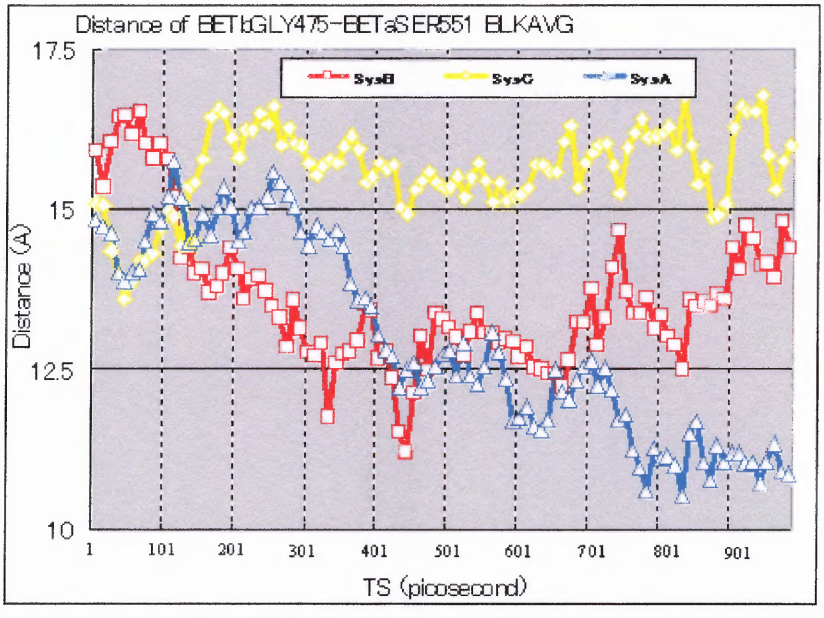

Figure G.3 Distance of β_{1_a} SER551 and β_{1_b} GLY475.

Table G.3 Distance Between β_{1_a} SER551 and β_{1_b} GLY475 in 1ns Simulation

	System A (Å)	System B (Å)	System C (Å)
300 ps simulation	14.8362	14.7005	15.3817
1 ns simulation	12.97815	13.62181	15.61517

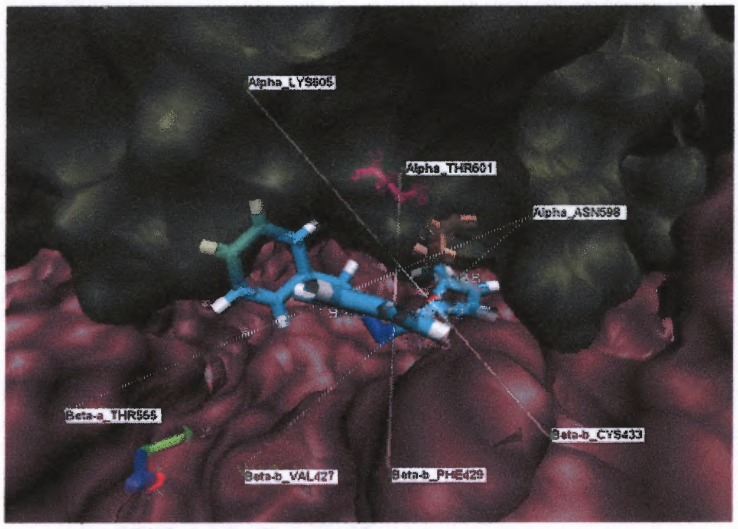

Figure G.4 Front end of YC-1 binding pocket.

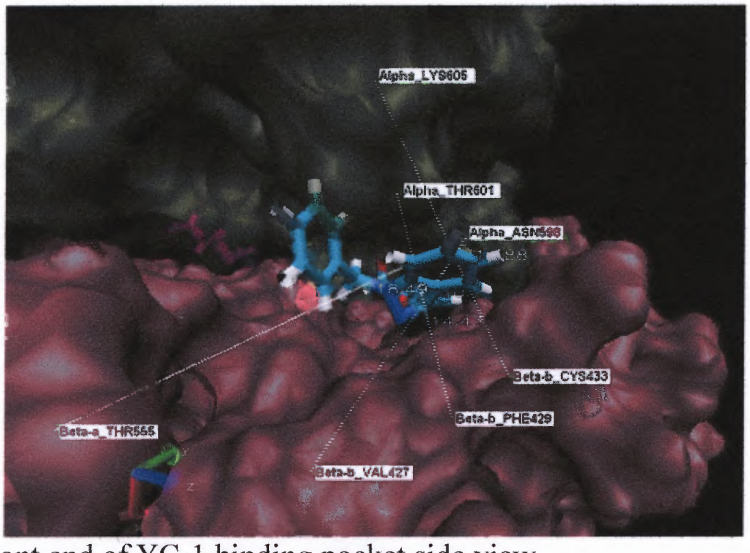

Figure G.5 Front end of YC-1 binding pocket side view.

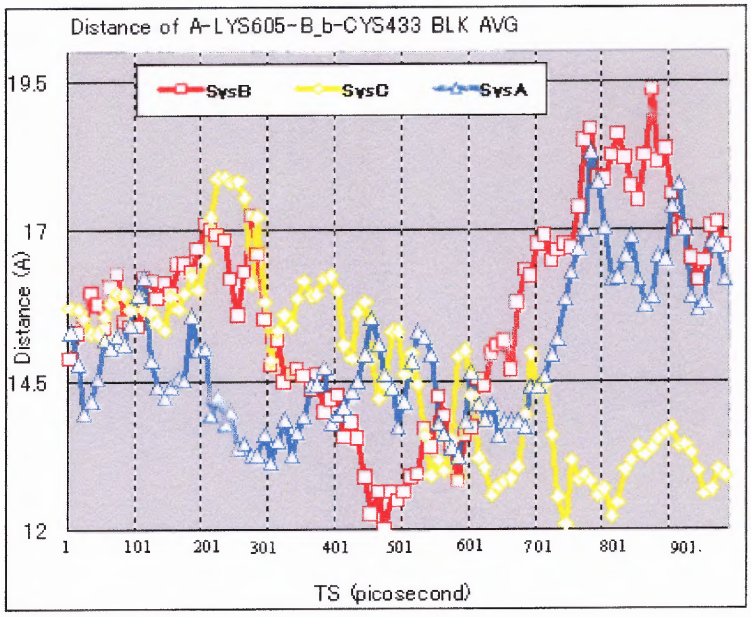

Figure G.6 Distance of α_1 LYS605 and β_{1_b} CYS433.

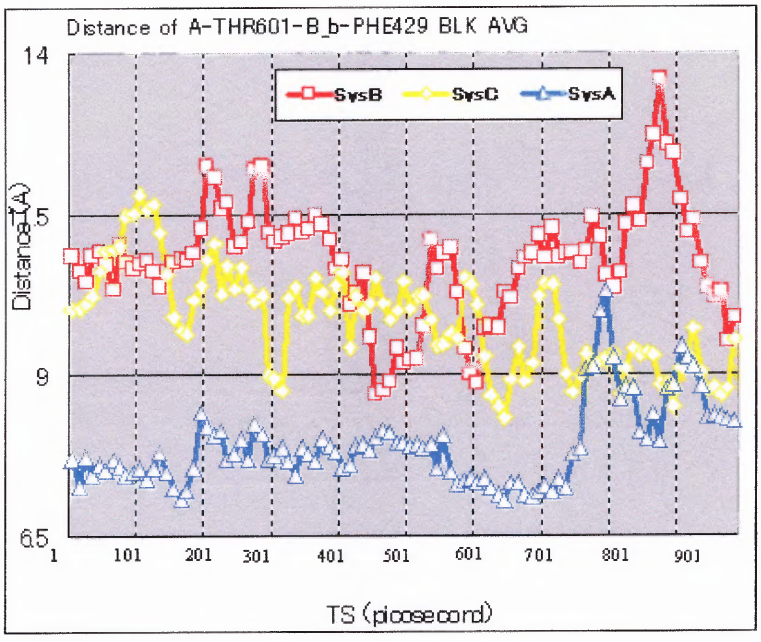

Figure G.7 Distance of α_1 THR601 and β_{1_b} PHE429

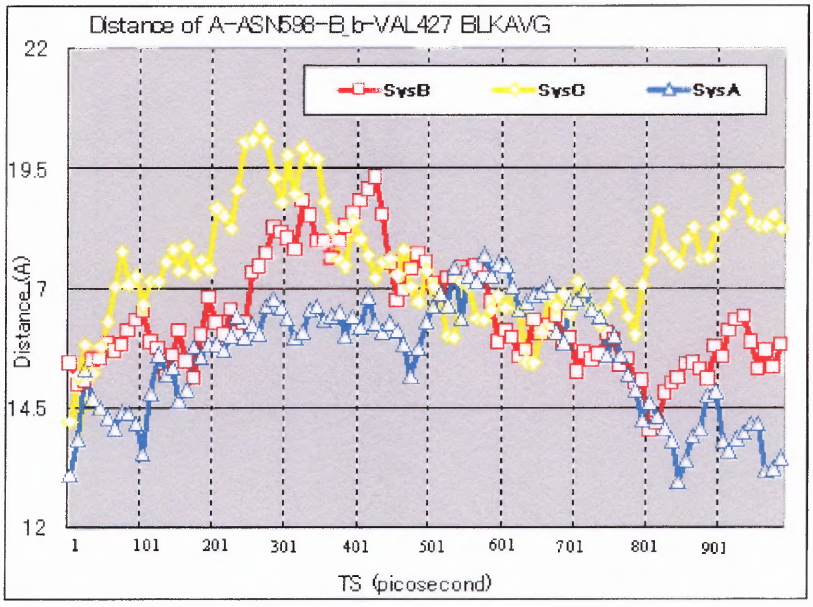

Figure G.8 Distance of α_1 ASN598 and β_{1_b} VAL427

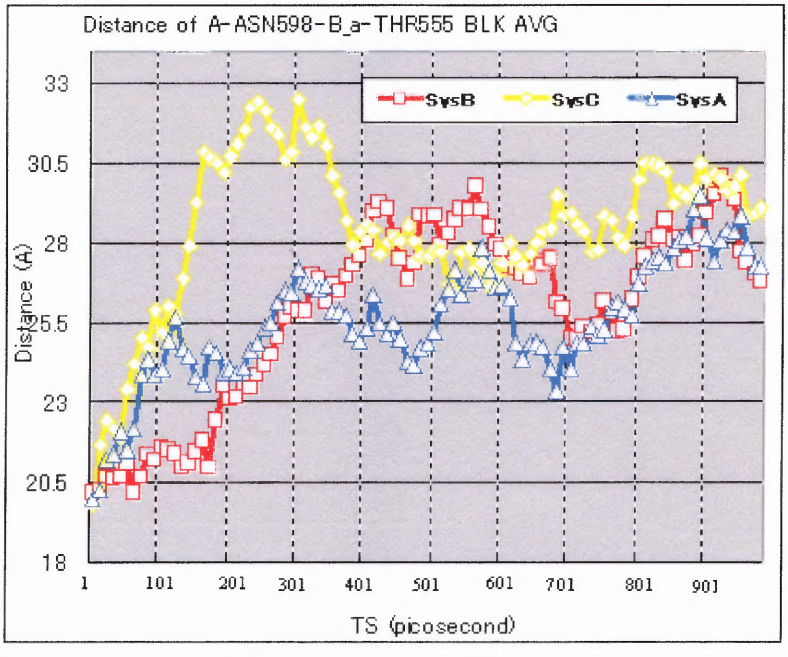

Figure G.9 Distance of α_1 ASN598 and β_{1_a} THR598

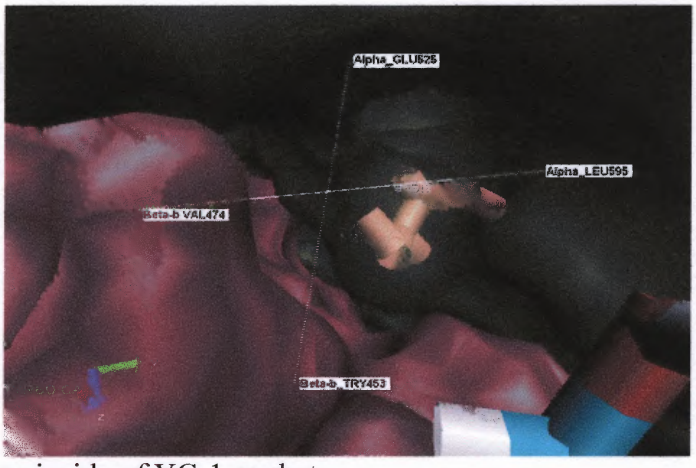

Figure G.10 Deep inside of YC-1 pocket.

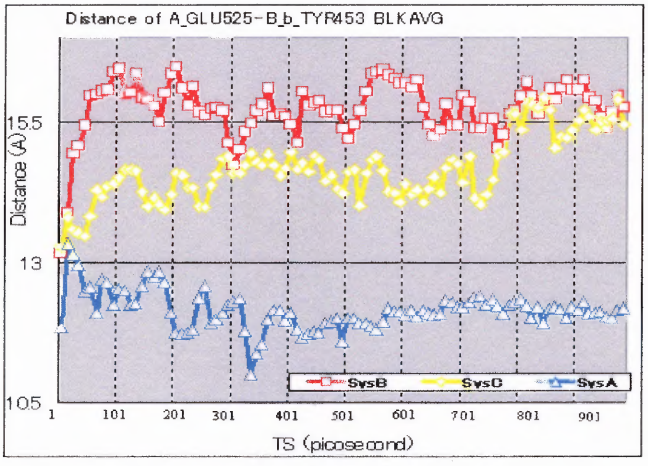

Figure G.11 Distance of α_1 GLU525 and β_{1_b} TYR453.

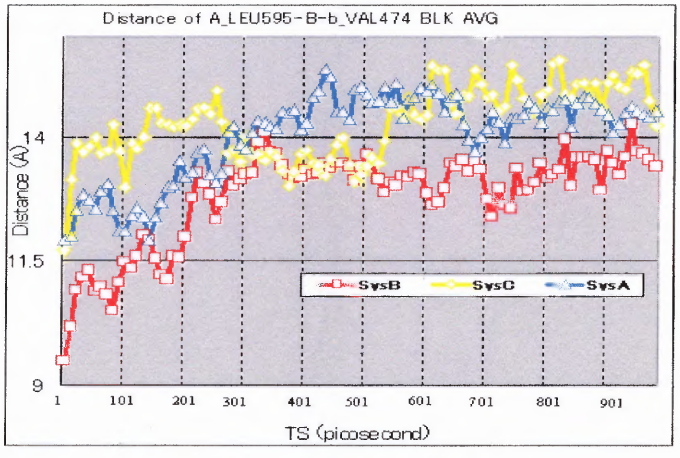

Figure G.12 Distance of α_1 LEU595 and β_{1_b} VAL474.

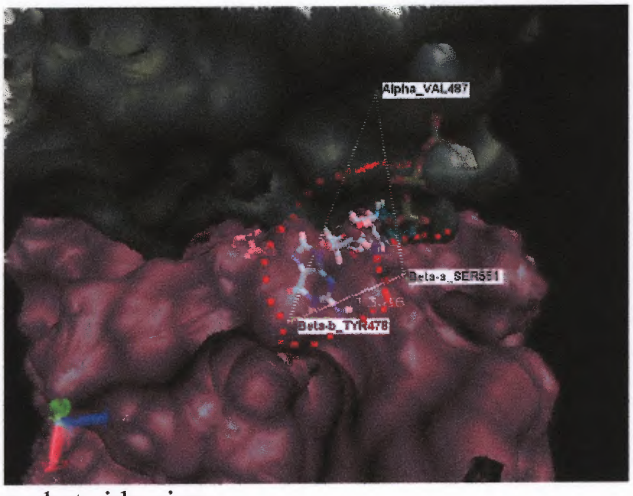

Figure G.13 GTP pocket side view.

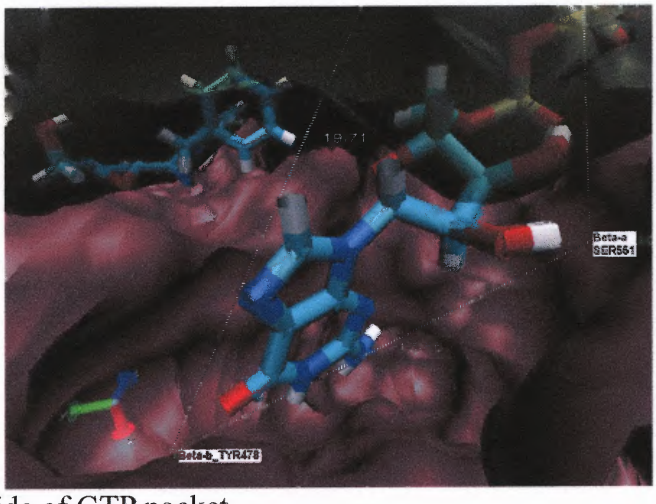

Figure G.14 Inside of GTP pocket.

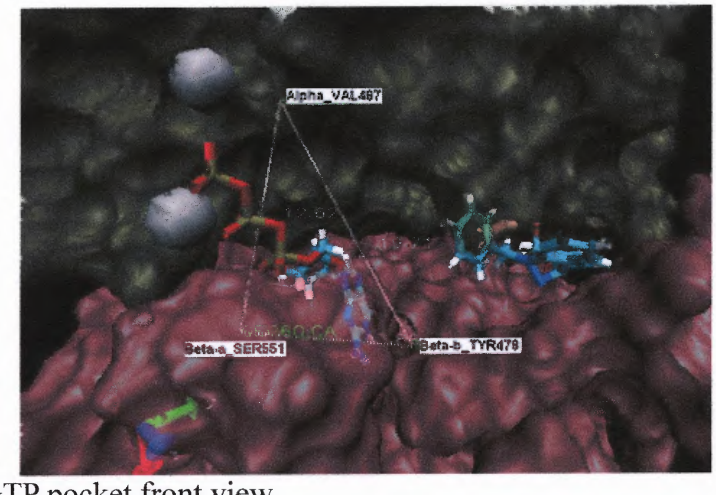

Figure G.15 GTP pocket front view.

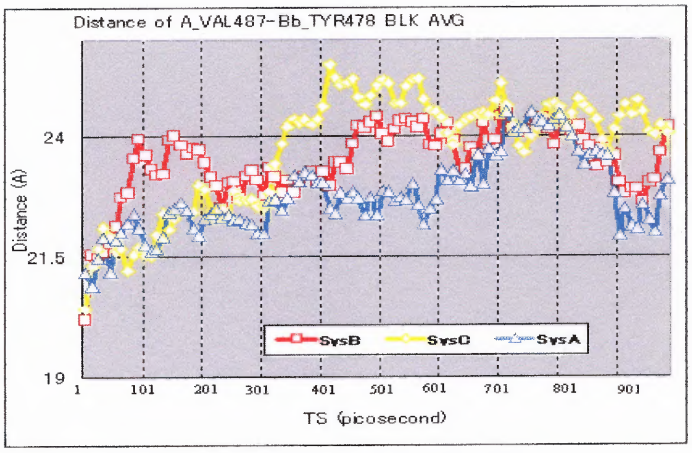

Figure G.16 Distance of α_1 VAL487 and β_{1_b} TYR478.

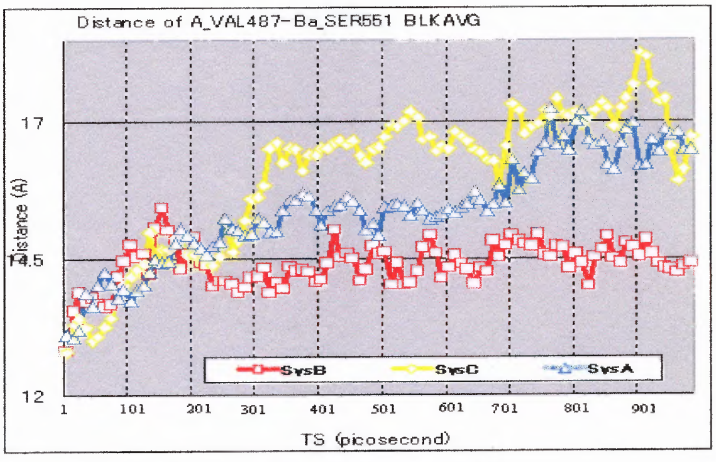

Figure G.17 Distance of α_1 VAL487 and β_{1_a} SER551.

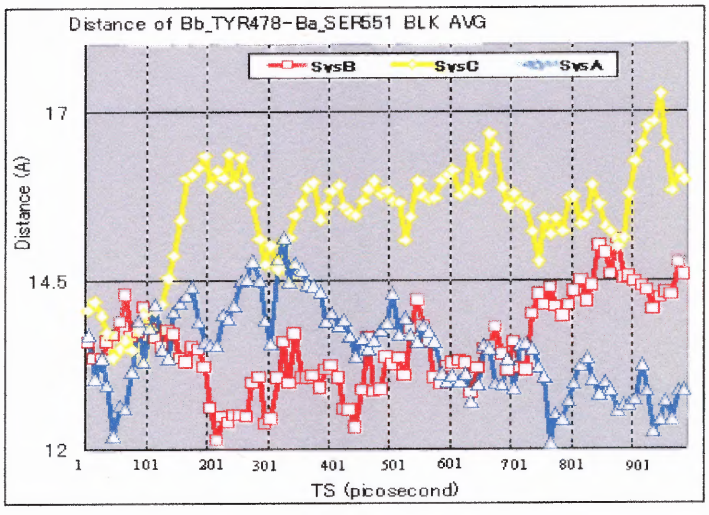

Figure G.18 Distance of β_{1_b} TYR478 and β_{1_a} SER551.

REFERENCES

1. Lamothe M., Chang F.J., Balashova N., Shirokov R., Beuve A.,
   "Functional characterization of nitric oxide and YC-1 activation of soluble guanylyl cyclase: structural implication for the YC-1 binding site?"
   Biochemistry. 43(11):3039-3048

2. A. Friebe, M. Russwurm, E. Mergia, and D. Koesling.,
   "A point-mutated guanylyl cyclase with features of the YC-1 stimulated enzyme: implications for the YC-1 binding site?,"
   Biochemistry, vol. 38, pp. 15253-15257, 1999.

3. J. Sopkova-de Oliveira Santos, V. Collot, I. Bureau, and S. Rault.,
   "YC-1, an activation inductor of soluble guanylyl cyclase,"
   Acta Crystallographica Section C, vol. 56, pp. 1035-1036, 2000.

4. P. E. Brandish, W. Buechler, and M. A. Marletta.,
   "Regeneration of the ferrous heme of soluble guanylate cyclase from the nitric oxide complex: acceleration by thiols and oxyhemoglobin,"
   Biochemistry, vol. 37, pp. 16898-16907, 1998.

5. R. Makino, H. Matsuda, E. Obayashi, Y. Shiro, T. Iizuka, and H. Hori.,
   "EPR characterization of axial bond in metal center of native and cobalt-substituted guanylate cyclase,"
   J. Biol. Chem., vol. 274, pp. 7714-7723, 1999.

6. T. Tomita, T. Ogura, S. Tsuyama, Y. Imai, and T. Kitagawa.,
   "Effects of GTP on bound nitric oxide of soluble guanylate cyclase probed by resonance Raman spectroscopy,"
   Biochemistry, vol. 36, pp. 10155-10160, 1997.

7. Laxmikant Kal Robert Skeel, Milind Bhandarkar, Robert Brunner, Attila Gursoy, Neal Krawetz, James Phillips, Aritomo Shinozaki, Krishnan Varadarajan, and Klaus Schulten.,
   "NAMD2: Greater scalability for parallel molecular dynamics,"
   Journal of Computational Physics, 151:283-312, 1999
   http://www.ks.uiuc.edu/Research/namd/

8. Humphrey, W., Dalke, A. and Schulten, K.,
   "VMD - Visual Molecular Dynamics,"
   J. Molec. Graphics, 1996, vol. 14, pp. 33-38.
   http://www.ks.uiuc.edu/Research/vmd/

9. Stewart, James J. P. J.,
"MOPAC,"
Comput. Aided Mol. Design 1990, 4, 1–105.

10. A. W. Schuettelkopf and D. M. F. van Aalten (2004).
"PRODRG - a tool for high-throughput crystallography of protein-ligand complexes. "
Acta Crystallogr. D60, 1355-1363.
http://davapc1.bioch.dundee.ac.uk/programs/prodrg/index.html
(accessed April 13. 2005).

11. M. Koglin, J. P. Stasch, and S. Behrends.,
"BAY 41-2272 activates two isoforms of nitric oxide-sensitive guanylyl cyclase,"
Biochem. Biophys. Res. Commun., vol. 292, pp. 1057-1062, 2002.

12. J. P. Stasch, E. M. Becker, C. Alonso-Alija, H. Apeler, K. Dembowsky, A. Feurer, R. Gerzer, T. Minuth, E. Perzborn, U. Pleiss, H. Schroder, W. Schroeder, E. Stahl, W. Steinke, A. Straub, and M. Schramm.,
"NO-independent regulatory site on soluble guanylate cyclase"
Nature, vol. 410, pp. 212-215, 2001.

13. P. Condorelli and S. C. George.,
"In Vivo Control of soluble guanylate cyclase activation by nitric oxide: a kinetic analysis."
Biophysical Journal, vol. 80, pp. 2110-2119, 2001.

14. E. Martin, Y.-C. Lee, and F. Murad.,
"YC-1 activation of humansoluble guanylyl cyclase has both heme-dependent and independent components,"
Proc. Natl. Acad. Sci. U.S.A., vol. 98, pp. 12938-12942, 2001.

15. J. H. Hurley.,
"The adenylyl and guanylyl cyclase super family,"
Curr. Opin. Struct. Biol., vol. 8, pp. 770-777, 1998.

16. Y. Liu, A. E. Ruoho, V. D. Rao, and J. H. Hurley.,
"Catalytic mechanism of the adenylyl and guanylyl cyclases: modeling and mutational analysis,"
Proc. Natl. Acad. Sci. U.S.A., vol. 94, pp. 13414-13419, 1997.

17. J. J. Tesmer, R. K. Sunahara, A. G. Gilman, and S. R. Sprang.,
"Crystal structure of the catalytic domains of adenylyl cyclase in a complex with GsGTPS,"
Science, vol. 278, pp. 1907-1916, 1997.

18. J. H. Hurley.,
"Structure, mechanism, and regulation of mammalian adenylyl cyclase,"
J. Biol. Chem., vol. 274, pp. 7599-7602., 1999.

19. R. K. Sunahara, J. J. Tesmer, A. G. Gilman, and S. R. Sprang.,
"Crystal structure of the adenylyl cyclase activator Gs,"
Science, vol. 278, pp. 1943-1947, 1997.

20. M. E. Hatley, B. K. Benton, J. Xu, J. P. Manfredi, A. G. Gilman, and R. K. Sunahara.,
"Isolation and characterization of constitutively active mutants of mammalian adenylyl cyclase,"
J. Biol. Chem., vol. 275, pp. 38626-38632, 2000.

21. Sharon Hammes-Schiffer.,
LECTURE NOTES
Computer Simulation of Organic and Biological Molecules
Chapter1 Introduction to Computer Simulation
Copyright (c) 1996, 1997 Professor Sharon-Hammes Schiffer, University of Notre Dame. All Rights Reserved
http://research.chem.psu.edu/shsgroup/chem647/newNotes/node1.html
(accessed April 13. 2005).

22. Yu Wang's website
HM of sGC
http://web.njit.edu/~yw6/HM%20of%20sGC.htm
(accessed April 13. 2005).

23. CHARMM Empirical Force Field
http://www.pharmacy.umaryland.edu/faculty/amackere/force_fields.htm
(accessed April 13. 2005).

24. Timothy Isgro, James Phillips, Marcos Sotomayor,Elizabeth Villa.,
NAMD TUTORIAL
http://www.ks.uiuc.edu/Training/Tutorials/namd/namd-tutorial.pdf
(accessed April 13. 2005).

25. Aaron Oakley, Timothy Isgro, Yi Wang.,
Topology File Tutorial
http://www.ks.uiuc.edu/Training/Tutorials/science/topology/topology-html/
(accessed April 13. 2005).

26. Rommie Amaro, Brijeet Dhaliwal, Zaida Luthey-Schulten.,
Parameterizing a Novel Residue
http://www.ks.uiuc.edu/Training/Tutorials/science/forcefield-tutorial/forcefield.pdf
(accessed April 13. 2005).

27. M.W.Schmidt, K.K.Baldridge, J.A.Boatz, S.T.Elbert, M.S.Gordon, J.J.Jensen, S.Koseki, N.Matsunaga, K.A.Nguyen, S.Su, T.L.Windus, M.Dupuis, J.A.Montgomery.,
GAMESS
J.Comput.Chem. 14, 1347-1363 (1993).

28. M. J. Frisch, G. W. Trucks, H. B. Schlegel, G. E. Scuseria, M. A. Robb, J. R. Cheeseman, J. A. Montgomery, Jr., T. Vreven, K. N. Kudin, J. C. Burant, J. M. Millam, S. S. Iyengar, J. Tomasi, V. Barone, B. Mennucci, M. Cossi, G. Scalmani, N. Rega, G. A. Petersson, H. Nakatsuji, M. Hada, M. Ehara, K. Toyota, R. Fukuda, J. Hasegawa, M. Ishida, T. Nakajima, Y. Honda, O. Kitao, H. Nakai, M. Klene, X. Li, J. E. Knox, H. P. Hratchian, J. B. Cross, V. Bakken, C. Adamo, J. Jaramillo, R. Gomperts, R. E. Stratmann, O. Yazyev, A. J. Austin, R. Cammi, C. Pomelli, J. W. Ochterski, P. Y. Ayala, K. Morokuma, G. A. Voth, P. Salvador, J. J. Dannenberg, V. G. Zakrzewski, S. Dapprich, A. D. Daniels, M. C. Strain, O. Farkas, D. K. Malick, A. D. Rabuck, K. Raghavachari, J. B. Foresman, J. V. Ortiz, Q. Cui, A. G. Baboul, S. Clifford, J. Cioslowski, B. B. Stefanov, G. Liu, A. Liashenko, P. Piskorz, I. Komaromi, R. L. Martin, D. J. Fox, T. Keith, M. A. Al-Laham, C. Y. Peng, A. Nanayakkara, M. Challacombe, P. M. W. Gill, B. Johnson, W. Chen, M. W. Wong, C. Gonzalez, and J. A. Pople, Gaussian, Inc., Wallingford CT, 2004.
Gaussian 03, Revision C.02.

29. P. Flükiger, H.P. Lüthi, S. Portmann, J. Weber.,
Swiss Center for Scientific Computing, Manno (Switzerland), 2000
MOLEKEL 4.0.

30. MOLDEN a pre- and post processing program of molecular and electronic structure.
http://www.cmbi.ru.nl/molden/molden.html
(accessed April 13. 2005).

31. Winmoster
http://winmoster.com/
(accessed April 13. 2005).

32. J. J. P. Stewart.,
"Optimization of Parameters for Semi-Empirical Methods I-Method."
J. Comp. Chem., 10:209-220, 1989.

32. A. Streitweiser Jr.,
Molecular orbital theory for organic chemists. New York:Wiley, 1961.

34. M. J. S. Dewar,
The molecular orbital theory for organic chemistry. New York:McGraw-Hill, 1969.

35. J. N. Murrell and A. J. Harget,
Semi-empirical self-consistent-field molecular orbital theory of molecules. London: Wiley, 1972.

37. T. A. Darden, D. M. York, and L. G. Pedersen,
"Particle mesh Ewald: A method for Ewald sums in large systems,"
Journal of Chemical Physics, vol. 98, pp. 10089-10092, 1993.

38. T. Schlick,
Molecular modeling and simulation: An interdisciplinary guide, vol. 21: Springer-Verlag New York, Inc., 2002.

39. Y. Duan and P. A. Kollman,
"Pathways to a protein folding intermediate observed in a 1-microsecond simulation in aqueous solution,"
Science, vol. 282, pp. 740-744, 1998.

40. Y. Duan, L. Wang, and P. A. Kollman,
"The early stage of folding of villin headpiece subdomain observed in a 200-nanosecond fully solvated molecular dynamics simulation,"
Proc. Natl. Acad. Sci. U.S.A., vol. 95, pp. 9897-9902, 1998.

41. M. Tuckerman, B. J. Berne, and G. J. Martyna,
"Reversible multiple time scale molecular dynamics,"
J. Chem. Phys., vol. 97, pp. 1990-2001, 1992.

42. H. Grubmöller, H. Heller, A. Windemuth, and K. Schulten,
"Generalized Verlet algorithm for efficient molecular dynamics simulations with long-range interactions,"
Molecular Simulation, vol. 6, pp. 121–142, 1991.

43. B. Honig and A. Nicholls,
"Classical electrostatics in biology and chemistry,"
Science, vol. 268, pp. 1144-, 1995.

44. Q. Ma, J. A. Izaguirre, and R. D. Skeel,
"Nonlinear instabilities in multiple time stepping molecular dynamics,"
in The 18th ACM Symposium on Applied Computing. FL, 2003, pp. 167-171.

45. Q. Ma, J. A. Izaguirre, and R. D. Skeel,
"Verlet-I/r-RESPA/Impulse is limited by nonlinear instability,"
SIAM J. Sci. Comput., vol. 24, pp. 1951-1973, 2003.